Transportation Consortium of South-Central States

Solving Emerging Transportation Resiliency, Sustainability, and Economic Challenges through the Use of Innovative Materials and Construction Methods: From Research to Implementation

UHPC Shear Keys in Concrete Bridge Superstructures

Project No. 18CNMS01

Lead University: New Mexico State University

Final Report

August 2019

Disclaimer

The contents of this report reflect the views of the authors, who are responsible for the facts and the accuracy of the information presented herein. This document is disseminated in the interest of information exchange. The report is funded, partially or entirely, by a grant from the U.S. Department of Transportation's University Transportation Centers Program. However, the U.S. Government assumes no liability for the contents or use thereof.

Acknowledgements

The authors would like to acknowledge the support and direction of the Project Review committee that included Dr. Paul Barr of Utah State University, Kathy Crowell of the New Mexico Department of Transportation, and Ken Wylie of Wood Plc.

TECHNICAL DOCUMENTATION PAGE

1. Project No.	2. Government Accession No.	3. Recipient's Catalog No.
18CNMS01		

4. Title and Subtitle	5. Report Date
UHPC Shear Keys in Concrete Bridge Superstructures	Aug. 2019
	6. Performing Organization Code

7. Author(s)	8. Performing Organization Report No.
PI: Craig M. Newtson https://orcid.org/0000-0002-2140-9759 Co-PI: Brad D. Weldon https://orcid.org/0000-0001-7196-8690 GRA: Elsy Flores https://orcid.org/0000-0001-7697-0247 GRA: Jordan Varbel https://orcid.org/0000-0003-4672-4138 GRA: William K. Toledo https://orcid.org/0000-0002-3436-5118	

9. Performing Organization Name and Address	10. Work Unit No. (TRAIS)
Transportation Consortium of South-Central States (Tran-SET) University Transportation Center for Region 6 3319 Patrick F. Taylor Hall, Louisiana State University, Baton Rouge, LA 70803	**11. Contract or Grant No.** 69A3551747106

12. Sponsoring Agency Name and Address	13. Type of Report and Period Covered
United States of America Department of Transportation Research and Innovative Technology Administration	Final Research Report Mar. 2018 – Mar. 2019
	14. Sponsoring Agency Code

15. Supplementary Notes

Report uploaded and accessible at Tran-SET's website (http://transet.lsu.edu/).

16. Abstract

This research investigated the use of locally produced ultra-high performance concrete (UHPC) as a grouting material to repair deteriorated shear keys. Shear keys are used in adjacent girder superstructures to produce monolithic behavior and load transfer across the structure. Shear key durability is a concern since shear key degradation can jeopardize the integrity of the structure. Transportation agencies have reported that 75% of distress in adjacent girder bridges is due to cracking and de-bonding along shear keys. Previous research has shown that locally produced UHPC has excellent mechanical and durability properties. UHPC has also been shown to have good bonding characteristics that are desirable in a potential grouting material. Several tests were conducted to evaluate the potential of UHPC as a shear key grout material. Bond strength between UHPC grout and substrate concrete was evaluated using slant-shear and direct tension tests. Results showed that adequate bond was achieved at seven days. However, 28-day strengths were less than recommended bond strengths. The low strengths were attributed to the low strength of the substrate concrete. Shrinkage of UHPC grout was also investigated. Total shrinkage was approximately 2000 μstrain with approximately half occurring in the plastic state. Full-scale testing was used to evaluate load-deflection behavior of channel girder assemblages with grouted shear keys. The results showed that UHPC grout and non-shrink grout had similar mechanical performance. Excellent bond was achieved with all grouts, even with minimal surface preparation. In fact, the shear keys remained bonded to the girders even when service load deflections were exceeded and no lateral restraint, such as post-tensioning, was provided. A non-shrink grout slightly outperformed the UHPC grout. While this outperformance of the non-shrink grout may not be significant, it does indicate that UHPC grout does not provide a mechanical benefit over the non-shrink grout.

17. Key Words	18. Distribution Statement
UHPC, Concrete, Grout, Shear Key, Bridge, Superstructure	No restrictions. This document is available through the National Technical Information Service, Springfield, VA 22161.

19. Security Classif. (of this report)	20. Security Classif. (of this page)	21. No. of Pages	22. Price
Unclassified	Unclassified	48	

Form DOT F 1700.7 (8-72) **Reproduction of completed page authorized.**

SI* (MODERN METRIC) CONVERSION FACTORS

APPROXIMATE CONVERSIONS TO SI UNITS

Symbol	When You Know	Multiply By	To Find	Symbol
		LENGTH		
in	inches	25.4	millimeters	mm
ft	feet	0.305	meters	m
yd	yards	0.914	meters	m
mi	miles	1.61	kilometers	km
		AREA		
in^2	square inches	645.2	square millimeters	mm^2
ft^2	square feet	0.093	square meters	m^2
yd^2	square yard	0.836	square meters	m^2
ac	acres	0.405	hectares	ha
mi^2	square miles	2.59	square kilometers	km^2
		VOLUME		
fl oz	fluid ounces	29.57	milliliters	mL
gal	gallons	3.785	liters	L
ft^3	cubic feet	0.028	cubic meters	m^3
yd^3	cubic yards	0.765	cubic meters	m^3
	NOTE: volumes greater than 1000 L shall be shown in m^3			
		MASS		
oz	ounces	28.35	grams	g
lb	pounds	0.454	kilograms	kg
T	short tons (2000 lb)	0.907	megagrams (or "metric ton")	Mg (or "t")
		TEMPERATURE (exact degrees)		
°F	Fahrenheit	5 (F-32)/9 or (F-32)/1.8	Celsius	°C
		ILLUMINATION		
fc	foot-candles	10.76	lux	lx
fl	foot-Lamberts	3.426	$candela/m^2$	cd/m^2
		FORCE and PRESSURE or STRESS		
lbf	poundforce	4.45	newtons	N
lbf/in^2	poundforce per square inch	6.89	kilopascals	kPa

APPROXIMATE CONVERSIONS FROM SI UNITS

Symbol	When You Know	Multiply By	To Find	Symbol
		LENGTH		
mm	millimeters	0.039	inches	in
m	meters	3.28	feet	ft
m	meters	1.09	yards	yd
km	kilometers	0.621	miles	mi
		AREA		
mm^2	square millimeters	0.0016	square inches	in^2
m^2	square meters	10.764	square feet	ft^2
m^2	square meters	1.195	square yards	yd^2
ha	hectares	2.47	acres	ac
km^2	square kilometers	0.386	square miles	mi^2
		VOLUME		
mL	milliliters	0.034	fluid ounces	fl oz
L	liters	0.264	gallons	gal
m^3	cubic meters	35.314	cubic feet	ft^3
m^3	cubic meters	1.307	cubic yards	yd^3
		MASS		
g	grams	0.035	ounces	oz
kg	kilograms	2.202	pounds	lb
Mg (or "t")	megagrams (or "metric ton")	1.103	short tons (2000 lb)	T
		TEMPERATURE (exact degrees)		
°C	Celsius	1.8C+32	Fahrenheit	°F
		ILLUMINATION		
lx	lux	0.0929	foot-candles	fc
cd/m^2	$candela/m^2$	0.2919	foot-Lamberts	fl
		FORCE and PRESSURE or STRESS		
N	newtons	0.225	poundforce	lbf
kPa	kilopascals	0.145	poundforce per square inch	lbf/in^2

TABLE OF CONTENTS

LIST OF FIGURES

LIST OF TABLES

ACRONYMS, ABBREVIATIONS, AND SYMBOLS

AASHTO	American Association of State Highway and Transportation Officials
ACI	American Concrete Institute
ASTM	American Society for Testing and Materials
CL1	Cyclic Loading 1
CL2	Cyclic Loading 2
CL3	Cyclic Loading 3
CL4	Cyclic Loading 4
FHWA	Federal Highway Administration
HRWRA	High-Range Water Reducing Admixture
LRFD	Load and Resistance Factor Design
LVDT	Linearly Variable Displacement Transducer
NM	New Mexico
NMDOT	New Mexico Department of Transportation
NMSU	New Mexico State University
PCI	Precast/Prestressed Concrete Institute
SCM	Supplementary Cementitious Material
SEM	Scanning Electron Microscopy
SSMTL	Structural Systems and Materials Testing Laboratory
TxDOT	Texas Department of Transportation
UHPC	Ultra-High Performance Concrete
VHPC	Very-High Performance Concrete

EXECUTIVE SUMMARY

The work presented in this report investigated the use of locally produced ultra-high performance concrete (UHPC) as a grouting material to repair deteriorated shear keys. Shear keys are used in adjacent girder superstructures to produce monolithic behavior and load transfer across the width of the structure. Shear key durability is a concern to engineers since shear key degradation can jeopardize the integrity of the structure. Transportation agencies have reported that 75% of distress in adjacent girder bridges is due to cracking along shear keys and de-bonding of the interfaces between the girders and the shear keys.

Previous research at New Mexico State University has shown that locally produced UHPC has excellent mechanical and durability properties. UHPC has also been shown to have good bonding characteristics that are desirable in a potential grouting material. Several tests were conducted to evaluate the potential of UHPC as a grout material. These tests included bond strength tests such as slant-shear and direct tensile strength tests, early-age and longer-term shrinkage tests to assess dimensional compatibility with substrate concrete, and full-scale tests to compare UHPC grouted shear keys with conventional non-shrink grout shear keys.

Bond strength between UHPC grout and normal strength concrete substrate was assessed using slant-shear and direct tension tests. Results from these tests showed that seven-day strengths for both bonded and textured surfaces exceeded recommended strengths from the American Concrete Institute for repair concrete of 1000 psi (7.0 MPa) for slant-shear bond strength and 150 psi (1.0 MPa) for direct tensile strength. However, 28-day strengths were less than the recommend strengths 2000 psi (13.8 MPa) for slant-shear strength and 250 psi (1.7 MPa) for direct tensile strength. The low strengths at 28 days were attributed to the low strength of the substrate concrete, which may have also have been compromised by cracks caused by chipping during surface preparation, since all of the slant-shear and direction tension fractures from textured specimens occurred in the substrate. The substrate was air-entrained, only wet-cured for seven days, and was tested at 28 days. It appears that the strength at 28 days was not capable of providing 2000 psi (13.8 MPa) shear strengths or 250 psi (1.7 MPa) tensile strengths.

Low strengths from formed surfaces tested at 28 days were even lower than seven-day strengths for the same surface. These results appear to be due to variation of the test results within the small population of specimens. However, it is also possible that shrinkage of the UHPC caused some dimensional incompatibility with the substrate that caused a slight loss of bond strength between seven and 28 days.

Shrinkage behavior of the UHPC grouting material was investigated using early-age and longer-term shrinkage tests. Two early-age shrinkage tests were conducted using UHPC beams with measurements recorded for seven days. Two sets of longer-term shrinkage specimens were tested to an age of 28 days. The total shrinkage strain during the 28-day period was approximately 2000 μstrain. Approximately 1000 μstrain of the shrinkage occurred during the first 10 hours when the UHPC was still plastic and was unlikely to transfer significant shear stress to the substrate concrete since the elastic modulus of the UHPC should be small at such early ages.

Full-scale testing was used to evaluate load-deflection behavior of channel girder assemblages with grouted shear keys. Tests were conducted on assemblages that used improperly bonded UHPC to grout a shear key with no surface preparation, a non-shrink grout in a prepared shear key, and UHPC grout in a prepared shear key. These tests were conducted to quantify the load-

deflection behavior and shear and moment distribution of the assemblages with different shear key grouting techniques.

Full-scale testing of the two channel girder assemblages with UHPC grouted shear keys demonstrated that the bond between the UHPC grout and the mature girders was able to withstand the maximum permissible deflection for an equivalent bridge. This occurred for formed shear key surfaces that provided improper bond (not pre-wetted) as well as full bond (pre-wetted) for the UHPC grout. Additionally, the excellent bond observed between the UHPC grout and the mature channel girders during full-scale testing occurred with no lateral restraint such as post-tensioning, and the shear keys remained bonded to the girders even when deflections of girders exceeded serviceability limits. This indicates that the bond strength between UHPC and mature substrate with a formed surface is not as great a concern as the bond strength results seemed to indicate.

The full-scale testing results also showed that the non-shrink grout appeared to slightly outperform the UHPC grout. While the structural performance of the non-shrink grout was only marginally better than the performance of the UHPC grout, it does indicate that the UHPC grout does not provide a mechanical benefit over the non-shrink grout. Therefore, if UHPC grout is selected for shear key applications, that decision should be based on durability and possibly economy.

1. INTRODUCTION

Precast girders are commonly used in North America due to their ease of construction, affordability, favorable aesthetic appeal, and high flexural stiffness. Some girder shapes require shear keys to ensure monolithic behavior and load transfer across the superstructure. However, shear key durability is a concern to engineers since shear key degradation can jeopardize the integrity of the structure. Transportation agencies have reported that 75% of distress in adjacent girder bridges was due to cracking along shear keys and de-bonding of the interfaces between the girders and the shear keys (*1).*

This study focuses on investigating the potential for using locally produced ultra-high performance concrete (UHPC) as a grouting material to rehabilitate shear keys in adjacent pre-stressed girder bridges in New Mexico, USA. The majority of UHPC research conducted to date has focused on proprietary mixtures. The use of local materials in non-proprietary UHPC mixtures provides an economical and sustainable alternative to proprietary products. Previous research at New Mexico State University (NMSU) has shown that locally produced UHPC has excellent mechanical and durability properties *(2)*. UHPC has also been shown to have good bonding characteristics *(3, 4)* that are desirable in a potential grouting material. In comparison to proprietary mixtures, locally produced UHPC has a decrease in cost of anywhere from 10 to 70% *(5)*. To evaluate UHPC for potential use as a grout in shear keys, bond between UHPC and normal strength concrete was studied, as well as shrinkage testing and full-scale testing of UHPC grouted shear keys.

2. OBJECTIVES

The overall objective of this study was to evaluate the potential of using a non-proprietary UHPC produced with local materials as a grouting material to repair deteriorated shear keys. The evaluation was performed by testing bond strength between UHPC and substrate concrete surfaces. Durability and effective long-term performance of a shear key greatly depends on the bond strength between the grout and the substrate material, differential shrinkage between the grout and the substrate, and cracking of the grouting material.

Slant shear and direct tension tests were performed to assess the bond strength between the substrate and the UHPC grout. These tests were performed on composite specimens with substrate textures that included a formed surface and chipped textures. Texture depths were quantified using ASTM E965 *(6*). The specific objective of this portion of the research was to assess the ability of UHPC produced with local materials to bond adequately to substrate concrete.

Scanning electron microscopy was used to characterize both bonded and fractured surfaces. The objective of this portion of the work was to look for evidence of favorable or problematic conditions at bonded interfaces.

Assessment of early-age and longer-term shrinkage of the UHPC was conducted to assess compatibility of the UHPC and the normal strength concrete substrate. The objective of this portion of the research was to consider shrinkage compatibility between the UHPC overlay and the substrate concrete in a manner that might illuminate insurmountable incompatibilities.

The final research task was full scale structural testing of precast channel girders with different grouting materials such as UHPC and non-shrink grouts. The objective of this task was to determine if the bond between the grouting materials and the precast girders was adequate to transfer shear and moment to an adjacent girder at full serviceability deflection, as well as to compare the performance of the grouting materials.

3. LITERATURE REVIEW

3.1. Ultra-High Performance Concrete

UHPC became commercially available in the US in 2000 *(7)*. That version of UHPC consisted of Portland cement, ground quartz, fine sand, an accelerating admixture, a high-range water reducing admixture (HRWRA), and 2% by volume of steel fibers *(1*). ASTM C1856 defines UHPC as having a compressive strength of 17,000 psi (120 MPa) *(8)*. Transportation agencies have reported compressive strengths greater than 30,000 psi (150 MPa) and sustained post-cracking tensile strengths greater than 720 psi (5 MPa) for some UHPC products *(7)*.

3.1.1. Properties of Ultra-High Performance Concrete

UHPC's properties are achieved through careful selection of its constituent materials to ensure optimized gradation and maximized packing density, as well as detailed preparation methods to properly mix and cure UHPC elements *(9)*. UHPC has a discontinuous pore structure that reduces liquid ingress and enhances durability *(7)*. Additionally, UHPC has low porosity, high density, excellent durability, and resistance to chemical and physical attacks *(7)*. UHPC's unique properties provide the potential to significantly improve the service life and durability of existing concrete bridge superstructures.

Another important characteristic of UHPC is that it exhibits excellent adhesive strength with a wide range of rough surfaces *(1)*. As a result, the durability of UHPC facilitates a lengthening of design life. UHPC has also been investigated for other applications such as: precast concrete piles, seismic retrofit of substandard bridge substructures, thin overlays, and security and blast mitigation applications.

Long-term properties of UHPC may be influenced by casting procedures since the dispersion and orientation of the fiber reinforcement is greatly influenced by placement methods. Some placement methods cause the fibers to show a preference for aligning in the direction of flow during casting. The ability of the fibers to remain in suspension is dependent on the rheology of the concrete. Consequently, an optimized gradation of granular materials should be targeted *(7)*.

3.1.2. Non-Proprietary Ultra-High Performance Concrete

One factor limiting adoption of UHPC is that many users are hesitant to use a new product. Therefore, they opt for conventional concrete materials. Another limitation is the higher cost of proprietary UHPC products compared to normal concrete *(10)*. Use of local materials in non-proprietary UHPC mixtures provides an opportunity to produce economical and sustainable alternatives to proprietary products. Although most UHPC research has focused on proprietary products, previous UHPC research at NMSU has shown that UHPC produced with locally available materials and supplementary cementitious materials (SCMs), such as silica fume and class F fly ash, exhibit comparable mechanical and durability properties to proprietary UHPC mixtures *(9, 11, 12)*. However, the incorporation of locally available materials can reduce materials cost up to 70% compared to proprietary UHPC *(5, 13)*.

3.1.3. Applications of Ultra-High Performance Concrete

In the United States, UHPC has been used in simple-span pre-stressed concrete girder bridges where the tensile strength was utilized to allow elimination of the mild steel reinforcing shear

stirrups. UHPC has also been used in deck bulb-double-tee girders to utilize the material's properties to facilitate accelerated construction to produce a desired rheological behavior *(7)*.

Over the past few years in the United States, the Federal Highway Administration (FHWA) has adopted UHPC as a new grouting material for connections between bridge components *(1)*. In 2009, UHPC was used to create deck-level connections between precast concrete elements in New York. In the first case, UHPC was used in transverse connections between precast deck panels. In another case, it was used in longitudinal connections between the top flanges of deck bulb-tee girders *(7)*. The use of UHPC in shear keys can improve the overall performance of a precast girder superstructure. Several studies have been conducted to evaluate shear keys grouted with UHPC. In Ontario, 42 box girder bridges have been built with UHPC shear keys since 2008 *(1)*.

3.1.4. Proprietary Ultra-High Performance Concrete

According to Haber et al. *(14)*, UHPC is a popular choice for bridge construction and rehabilitation applications in North America. To promote this novel material, the FHWA launched an experimental study on six proprietary UHPC-class mixtures *(14)*. The study concluded that UHPC had a final setting time of seven to 24 hours, achieved compressive strengths greater than 14 ksi (97.5 MPa) within seven days without wet curing, and split-cylinder tests showed that UHPC exhibited the same first cracking strength of approximately 1.0 ksi (6.9 MPa), regardless of fiber volume *(14)*. Direct tension tests on UHPC and precast concrete composites showed that UHPC exhibited good bond, indicated by the failure stress at the bond interface occurring at approximately the same stress as the substrate at failure. UHPC mixtures tended to experience greater autogenous shrinkage than normal concrete, which can be attributed to the high cementitious materials contents in UHPC mixture proportions.

3.2. Shear Keys between Superstructures

Shear keys are critical structural components of a bridge superstructure. They are located between adjacent girders and are designed to restrain lateral displacement and facilitate load transfer between the girders. Figure 1 shows a shear key configuration in a bridge superstructure. The durability of shear keys is also a concern to researchers and engineers *(1)*. Shear key degradation can include de-bonding, cracking, and leaking that can compromise the strength and serviceability of the bridge. As a result, beams will not deflect equally under live loads. Differential displacement between girders may result in cracking in overlays and in the shear keys *(15)*. When leakage occurs, water with deicing salts can more easily penetrate to the reinforcement and pre-stressing strands to cause corrosion of the steel *(16)*.

Knowing that a direct correlation exists between load distribution and service life, several geometric configurations and grouting materials have been studied to improve shear key performance. Some configurations have included the design of a shear key at partial, medium, and full depth. Grouting materials, such as non-shrink grout, epoxy grout, engineered cementitious composites, and UHPC, have also been investigated *(17)*.

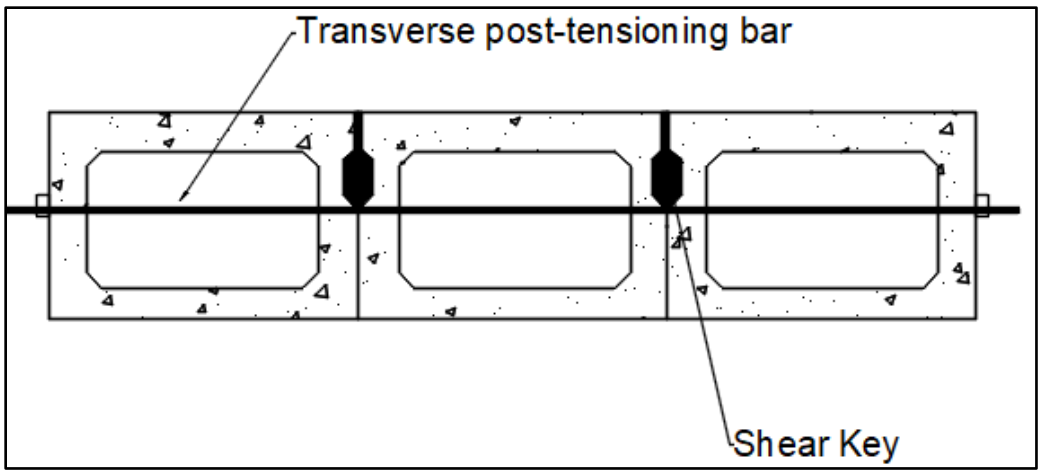

Figure 1. Superstructure cross-section with shear keys and post-tensioning.

3.2.1. Longitudinal Cracking

Longitudinal or reflective cracking along shear keys is an important concern among engineers because it requires maintenance and repair of bridge superstructures. Sharpe *(18)*, used finite element models to compare stresses in bridges with Texas Department of Transportation (TxDOT) girder designs with Precast/Prestressed Concrete Institute (PCI) girder designs. It was concluded that both girder types experienced uneven temperature changes and a lot of shrinkage that led to high tensile stresses at the interface between the girders and the shear keys. Consequently, cracking along the shear keys occurred. The stresses were greatest at the supports. Cracking can also occur if the shear keys are only designed to resist vertical shear if there are other types of stresses acting on the bonded interface, such as transverse normal stress from shrinkage, thermal effects, and wheel loads *(18)*.

To reduce tensile stresses, researchers have studied the incorporation of composite deck slabs and transverse post-tensioning on the stress field in the shear key. Results of that work show that reduced tensile stresses produce less reflective cracking. Studies have shown that the best way to solve reflective cracking includes using: a larger composite deck slab, full-depth shear keys, and adequate transverse post-tensioning. Of these options, the thicker composite deck slab is the most effective way to reduce stresses in the shear key. Some states, such as Texas, have increased their minimum reinforced deck slab to five inches, while other states have more extensive transverse post-tensioning *(18)*.

TxDOT and other DOTs have reported longitudinal cracks at the shear keys to be so severe that an entire bridge could potentially need to be replaced. It can be a major maintenance issue. Shear keys deteriorate over time due to repetitive traffic loads. Cracks allow water and deicing salts to corrode steel, such as the bar for the post-tensioning and tie bars if present. If a shear key is damaged, one or more girders can be overloaded due to lack of adequate load distribution *(18)*.

3.2.2. Transverse Post-Tensioning

Transverse post-tensioning improves load transfer across shear keys by creating a more monolithic behavior *(15)*. Post-tensioning also protects the bond between the shear key grout and a girder by keeping the bonded interface compressed. Other studies have shown that the post-tensioning force

required to ensure monolithic behavior is dependent on the width of the bridge and the depth of the girder *(19, 20).*

Research on Transverse Post-Tensioning: Post-tensioning has the ability to reduce tension failures by applying transverse compression across the shear keys, the amount of force and spacing of the post-tensioning strands needed are not well understood. Studies have shown that having evenly distributed transverse post-tensioning improves the performance of the bridge system. However, general practice uses transverse post-tensioning through the end and mid-span diaphragms. This practice does produce a uniform compression force along the length of the shear key. Consequently, post-tensioning may not always delay crack formation and propagation *(15)*. Post-tensioning can also increase cost and make the superstructure more complicated *(18)*.

Another study applied a Japanese method for repairing shear keys in the United States *(21)*. This method consists of making the deck act as a rigid assembly of longitudinal and transverse members. The idea was to use full-depth shear keys with a cast-in-place filled diaphragm at the quarter point locations of the bridge where high force post-tension strands were used. That work concluded that the post-tensioning force needed is constant per unit length along the span *(21)*.

Factors Affecting Post-Tensioning: Another study relating strength of shear keys to the amount of transverse post-tensioning evaluated shear key strength and behavior by conducting push off tests (direct shear tests on shear couplets). Based on the findings, the author was able to develop an empirical formula to calculate the shear strength of post-tensioned shear keys. This formula relates pre-stressing force across the connection with compressive strength of the grout material. It was concluded that the shear strength of the connection increases with increasing levels of post-tensioning and that shear strength is not dependent on the distribution of post-tensioning along the height of the connection *(22)*.

Most shear key cracking in adjacent beam bridges is due to temperature gradient and that the minimum force needed for transverse post-tensioning increases as the bridge width increases. This is a logical conclusion because as the width of the bridge increases so do the thermal effects. Furthermore, engineers have concluded that while the necessary transverse post-tensioning is dependent upon bridge width, it is independent of girder width *(19)*.

The required transverse post-tensioning force is also dependent upon the depth of the girders. In fact, when shallow girders are used, bridge length and skew angle can cause an increase in the required transverse post-tensioning. It is important to note that using the load resistance factor design (LRFD) method results in post-tensioning forces up to 40% greater than previous design methods *(20)*.

3.3. Bond of Repair Concrete

De-bonding is one of the main causes of shear key failure. Lack of bond allows water infiltration that can accelerate degradation of the concrete and embedded reinforcement *(23)*. Furthermore, bonding between shear key grout and a girder is important to ensure that a crack does not occur along the edge of the beam at the joint. Studies have shown that UHPC has high bond strengths affected primarily by the strength and surface preparation of the existing beam surface *(4)*.

Preparation of the surface of a precast member must be adequate to ensure long-term performance of the system. UHPC may not form a strong bond with smooth dry, precast concrete. Therefore, a surface exposing some micro- and macro-texture can result in better bond. Two ways to produce

a good bond between UHPC and precast concrete is pre-wetting the precast concrete to a saturated surface dry condition before placement of UHPC. This eliminates the dehydrating effect that occurs when the dry concrete extracts moisture from the UHPC. It is also useful to roughen the surface or provide an exposed aggregate finish *(15, 24).*

To prepare the surface of the substrate concrete, the old grouting material must be removed, and the precast member should be cleaned. The best practice for removal of deteriorated concrete is accomplished by scarification. Scarifying the substrate makes abrasions in the substrate and removes loose material. It is important to remove coatings or contaminants from the surface because they can break the bond between the substrate and the grouting material. Four common mechanisms used to remove damaged concrete are presented in ICRI 310's guidelines for selecting and specifying concrete surface preparation *(25).* The four methods of scarification are impact, abrasion, pulverization, and high-pressure water erosion.

3.3.1. Impact

This method of scarification uses impact tools such as rotary or demolition hammers. The impact method is the most economically feasible and time efficient method for surface preparation. The drawback of using this method is the possibility of introducing micro-cracks in the substrate concrete *(25).*

3.3.2. Abrasion

Grinding stones or discs are used for the abrasion scarification method. Although this is a scarification method, abrasion is best for smoothing the surface rather than providing a textured surface that will contribute to bond strength between a grout and substrate concrete *(25)*. Grinding of the surface with a rotary grinder leaves little to no surface profile.

3.3.3. Pulverization

Steel shot-blasting and sand blasting are examples of the pulverization scarification method. The pulverization method is a good way to texture a surface that has a low risk of producing micro-cracks *(25)*. This method requires the use of compressed air mixed with an abrasive material.

3.3.4. High-Pressure Water Erosion

Hydro-demolition (high-pressure water erosion) is widely considered to be the best practice for achieving scarification. Just like the pulverization scarification method, hydro-demolition can provide sufficient texturing of the substrate. This method also does not cause micro-cracks in the substrate material *(25)*. Hydro-demolition tools supply a water pressure against the substrate of 12,000 to 35,000 psi (83 to 241 MPa).

3.4. Grouting Materials

While the depth of the shear keys plays a role in durability, so does the grouting material. Grouting materials can be categorized as: commercially produced or developed by state transportation agencies. Common properties that exist among the different types of grouting materials are a relatively high strength at a young age, little shrinkage deformation, superior bonding with hardened concrete surfaces, and low permeability *(26)*.

3.4.1. Polymer Grout

Grouted joints between concrete panels do not perform well under large repetitive loadings. In past research, engineers tested several different grouting materials. Different specimens were tested for vertical shear, direct tension, and flexural capacity. It was concluded that polymer grout was the best choice as a grouting material for transverse joints due to its high strength. The more expensive polymer was also recommended when a joint is subjected to high stresses or when opening to traffic at an early age is critical *(27)*.

3.4.2. Epoxy Grout

Tests have also been conducted on shear keys located near the top of beams using epoxy grout rather than conventional non-shrink grout *(28)*. In that study, the shear keys had no cracking after curing. Beams were tested to one million cycles and then observed for four weeks to analyze the temperature effects on the shear keys. It was found that the epoxy did not crack. This was attributed to the superior bond strength of the epoxy grout compared to non-shrink grout. It was noted that epoxy grouted shear keys can be a non-desirable option due to the inability to repair the keys without causing serious damage to the girders *(28)*.

3.4.3. Conventional Non-Shrink Grout

Another study tested using conventional non-shrink grout and a commercially available mortar that has been adopted by many DOT's in the US and Canada. To provide a worst-case scenario, the substrate surface was left outside to produce a carbonated surface. When direct tension tests were performed, the composite specimen failed in the substrate (loads that produce failure in the substrate are the maximum attainable) for the mortar, while for the non-shrink grout failure occurred at the bonded interface. When tested in vertical shear, failure occur at the bonded interface for the non-shrink grout and cracks occurred in the both the substrate and bonded interface for the mortar *(29)*.

3.4.4. Very-High Performance Concrete Grout

Further research on grouting materials for shear keys compared non-shrink grout, UHPC, and very-high performance concrete (VHPC) as shear key grouting materials within voided slab bridges. The UHPC was a proprietary mixture, Ductal®, produced by LaFarge, while the VHPC was a non-proprietary mixture designed at Virginia Polytechnic Institute and State University. After the specimens were cyclically tested, it was found that while all three did crack, UHPC and VHPC outperformed the non-shrink grout in terms of bond and compressive strength. When comparing the UHPC and VHPC, it was concluded that the VHPC was the best option because it was more economical *(30)*. This conclusion was similar to observations by Hussein et al. (*31)* who performed direct shear, direct tension, and flexural tests on UHPC shear keys. The results showed that without shear reinforcement, the cracking threshold and ultimate shear strength of UHPC shear keys were greater than for any other grouting material or configuration.

3.5. Testing Methods

To assess shear and tensile strengths of the bond interface, mechanical tests are typically conducted. Three types of failure can occur: de-bonding, material failure, or a combination of de-bonding and material failure. The most likely to occur is de-bonding, regardless of the different loading conditions. A shear key with a cementitious grout material will not achieve its full strength if it de-bonds from the face of the beam prematurely *(18)*.

3.5.1. Small-Scale Testing

Small-scale testing has been performed by various researchers to characterize the bond strength of different shear key grouts tested in shear, flexure, and tension. To assess shear and tensile strengths of the bond interface, it is common to perform slant-shear tests, split cylinder or split prism tests, and direct tension tests.

The slant-shear test is a widely used test to assess the bond shear strength between the substrate and repair concrete by inducing a combination of compressive and shear stresses *(21, 22)*. ASTM C882 / C882M *(32)* is a standard slant-shear test method for testing epoxy resin bond strength between two concrete specimen halves that is commonly used to assess bond strengths for repair concrete *(23).*

Two methods to assess tensile strength of the bond are commonly used. These two tests are the pull-off test and the split-cylinder test *(22)*. The pull-off test consists of partially coring an overlaid specimen and applying a tensile force until fracture occurs *(22*). ASTM C1583 provides a specification for performing this test *(33).*

3.5.2. Strength Recommendations

The minimum recommended bond strengths for repair materials for the direct tension test are 150 psi (1.0 MPa) at seven days and 250 psi (1.7 MPa) at 28 days. For the slant shear test, the minimum recommended shear strengths are 1000 psi (6.90 MPa) at seven days and 2000 psi (13.8 MPa) at 28 days *(24).*

3.5.3. Full-Scale Testing

One advantage of full-scale testing over small scale testing is that the former can be tested in a manner similar to how shear keys will be used in the field. On the other hand, two disadvantages are that determining the type of failure in the shear key is difficult and full-scale testing is expensive *(15).*

4. METHODOLOGY

The following sections present details regarding the UHPC mixture, proportions used for the substrate material, and the methods used to perform the bond strength tests, shrinkage tests, and large-scale girder testing.

4.1. Mixture Proportions

The UHPC mixture consisted of Type I/II Portland cement, silica fume, fly ash, HRWRA, water, and 2% steel fibers by volume. The sand, cement, and fly ash were obtained from local sources, and the silica fume, steel fibers, and HRWRA were obtained from regional suppliers.

The substrate concrete mixture used in the laboratory investigation consisted of Type I/II Portland cement, fine and coarse aggregates, water, and air-entraining admixture. Tables 1 and 2 present the mixture proportions for the UHPC and substrate concrete mixtures.

Table 1. Non-proprietary UHPC mixture proportions.

Material	Cement	Silica Fume	Fly Ash	Sand	HRWRA gal/yd^3 (L/m^3)	Water	Steel Fibers
lb/yd^3 (kg/m^3)	1377 (817)	172 (102)	172 (102)	1702 (1009)	9.09 (45)	258 (153)	201 (119)

Table 2. Substrate concrete mixture proportions.

Materials	Cement	Coarse Aggregate	Sand	Water	Air-Entraining Admixture fl oz./yd^3 (L/m^3)
lb/yd^3 (kg/m^3)	580 (344)	1660 (985)	1212 (719)	290 (172)	29 (1.22)

4.2. Compressive Strength Tests

Compressive strength tests were performed to characterize the UHPC and normal strength concrete used in the bond strength tests. The compressive strength of the UHPC was tested using 3.94 in. (100 mm) cube specimens. Seven and 28-day compressive strength tests were conducted for the compressive strength of the UHPC according to BS 1881 since there is no ASTM specification for compressive strength testing of cast cube specimens *(34)*.

The compressive strength of the normal strength concrete was tested according to ASTM C39 using 6x12 in. (152x305mm) cylinder specimens *(35)*. Seven- and 28-day compressive strength tests were also conducted for the compressive strength of the normal strength concrete.

4.3. Bond Strength Tests

Specimens were produced by casting the substrate, moist curing the substrate to an age of seven days, casting the UHPC portion of the specimen, and then curing at ambient conditions (68°F [20°C] and relative 30% humidity) until the specimens were tested at either seven or 28 days.

Slant-shear and direct tension tests were performed to assess the bond strength between the UHPC grout and the substrate concrete. These tests were performed on composite specimens with substrate textures that included a formed surface and chipped textures with depths that ranged from 0.008 to 0.13in (0.203 to 3.302mm).

4.3.1. Slant-Shear

The slant-shear tests conducted for this work followed ASTM C882 which addresses testing epoxy resin bond strength between two concrete specimen halves *(32)*. In this study, bonding agents were not used to adhere the UHPC grout to the substrate material. Consequently, the bond strength, which relies on the pozzolanic nano-particles in the UHPC, was assessed.

Slant-Shear Setup: Specimen preparation deviated slightly from ASTM C882 in that the normal strength concrete substrate was cast in a 6 by 12 in (152 by 304 mm) cylindrical mold. The mold uses a plastic dummy insert to produce a 60° incline. Figure 2 illustrates the slant-shear casting setup. The specimens were moist cured for seven days prior to texturing (if needed) and placement of UHPC. After de-molding, the composite specimens were cured at ambient conditions (68°F [20°C] and 30% relative humidity). The specimens were tested in compression to determine the shear strength of the bond at either seven or 28 days.

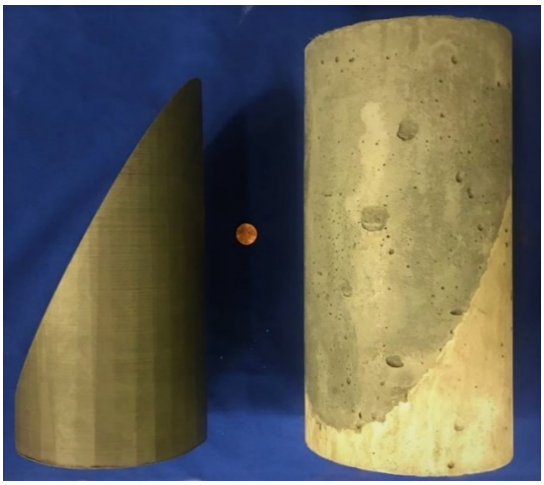

Figure 2. Slant-shear substrate casting set-up.

Surface Preparation: Texture depth was determined in accordance with ASTM E965 *(6)*. Surface preparation varied from formed to medium roughness. The formed surface was prepared by using a stiff wire brush to dust off loose material and the chipped surfaces were prepared by using an air hammer to chip off the formed surface. Figure 3 illustrates three of the substrate textures.

Figure 3. Substrate textures: formed, 0.06 in. (1.52 mm), and 0.10 in. (2.54 mm).

Slant-Shear Testing: The slant-shear specimens were tested in compression, as shown in Figure 4, until failure. Three possible failure modes can occur that include failure in the UHPC, failure of the bond, and failure in the substrate. Shear strength of the bond was calculated using the following equation:

$$\tau_n = \frac{P}{A}\sin(\alpha)\cos(\alpha) \qquad [1]$$

where:
τ_n = Shear stress (psi);
P = Ultimate load (lb);
A = Cross sectional area (in^2); and
α = Angle of the bonded interface from horizontal (60°).

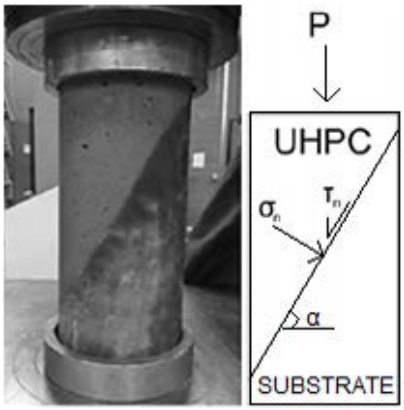

Figure 4. Slant-shear test setup.

4.3.2. Direct Tension

Direct tensile strength of bonded specimens was evaluated using a modified version of ASTM C1583 *(32).* The standard test uses a pull-off device to determine the strength from cored slabs. For this research, that device was replaced with the tension test apparatus shown in Figure 5 to test cylindrical cores taken from prismatic specimens.

Direct Tension Setup: The substrate material was cast using a 3x4x16 in. (76x102x406 mm) beam mold filled half-way with normal strength concrete. After 24 hours, the substrate material was placed in a moist room (73°F [23°C] and 98% relative humidity) for seven days to cure. After seven days, the UHPC was applied and left to cure at ambient conditions (68°F [20°C] and 30% relative humidity) for seven days. Six days after the UHPC was applied, 1.875 in. (47.6 mm) specimens were cored from the beam as shown in Figure 6. The specimen was then bonded to end plates using epoxy. Direct tension tests were conducted seven days and 28 days after the UHPC was applied to the substrate.

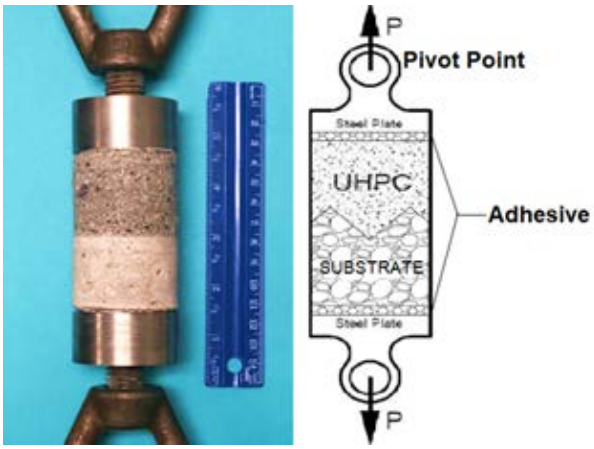

Figure 5. Direct tension test setup.

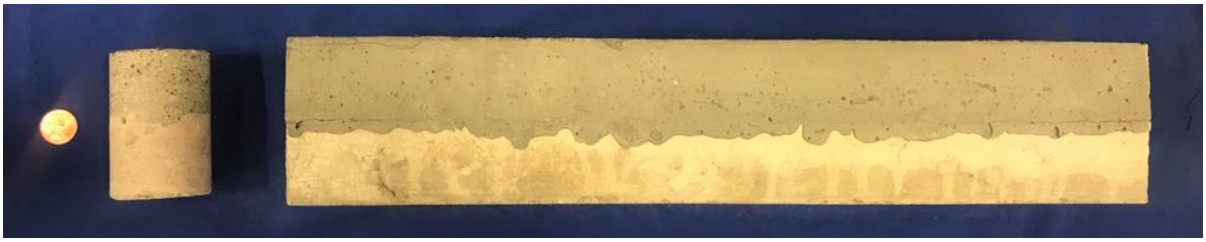

Figure 6. Direct tension specimen preparation.

Surface Preparation: The normal strength concrete substrate was textured in the same manner as the slant-shear specimens to achieve the same texture depths (Figure 3).

Direct Tension Test: Figure 5 illustrates the attachment of eye-bolts to the end plates epoxied to the specimen. The eye-bolts served as pivots at both ends of the specimen during loading so that concentric loading was ensured. The bond strength was calculated by using the ultimate load during testing in Equation 2:

$$T = \frac{P}{A_c} \qquad [2]$$

where:
T = tensile strength (psi);

P = ultimate load (lb); and
A_c = cross-sectional area of the specimen (in^2).

4.4. Shrinkage Testing

4.4.1. Early-Age Shrinkage

Shrinkage in the UHPC is important because it will cause shear and tensile stresses on the bond between the shear key grout and the mature substrate concrete. If the shrinkage is excessive, the combination of shear and tensile stresses can cause cracking at the bonded interface, which would lead to degradation of the shear key.

Early-Age Shrinkage Setup: No standard test specifications are available for early-age shrinkage testing, so a test method developed by *(36)* was adopted. This test method was used for previous research at NMSU *(12, 37).* The early-age shrinkage specimen was a 6x6x24 in. (152x152x610 mm) UHPC beam. The testing apparatus consisted of a steel frame that was placed over the mold for the UHPC shrinkage specimen so that it spanned the mold in the longitudinal direction. The beam mold was lined with plastic, talc powder, and another layer of plastic to minimize friction between the UHPC shrinkage specimen and the beam mold. As the UHPC shrinkage specimen was cast, steel hangers supported by the steel frame were embedded into the UHPC beam to a depth of 1 in. (25 mm) at a location that was 1 in. (25 mm) from the ends of the beam mold. Linearly variable displacement transducers (LVDTs) that were supported by the steel frame were used to monitor movement of the hangers caused by shrinkage. A photograph of the experimental setup for the early-age shrinkage test is presented in Figure 7.

Early-Age Shrinkage Test: The early-age shrinkage test ran for seven days with LVDT readings collected every 15 seconds. The gage length of the specimen was 22 in. (559 mm), from hanger to hanger. The change in length of the specimen was computed using the measurements of the two LVDTs shown in Figure 7. Changes in length obtained from the LVDT measurements were used in Equation 3 to calculate the shrinkage strains in the UHPC.

$$\varepsilon = \frac{\Delta L}{L} \qquad [3]$$

where:
ε = Strain;
ΔL = Change in length (in); and
L = Gage length (in).

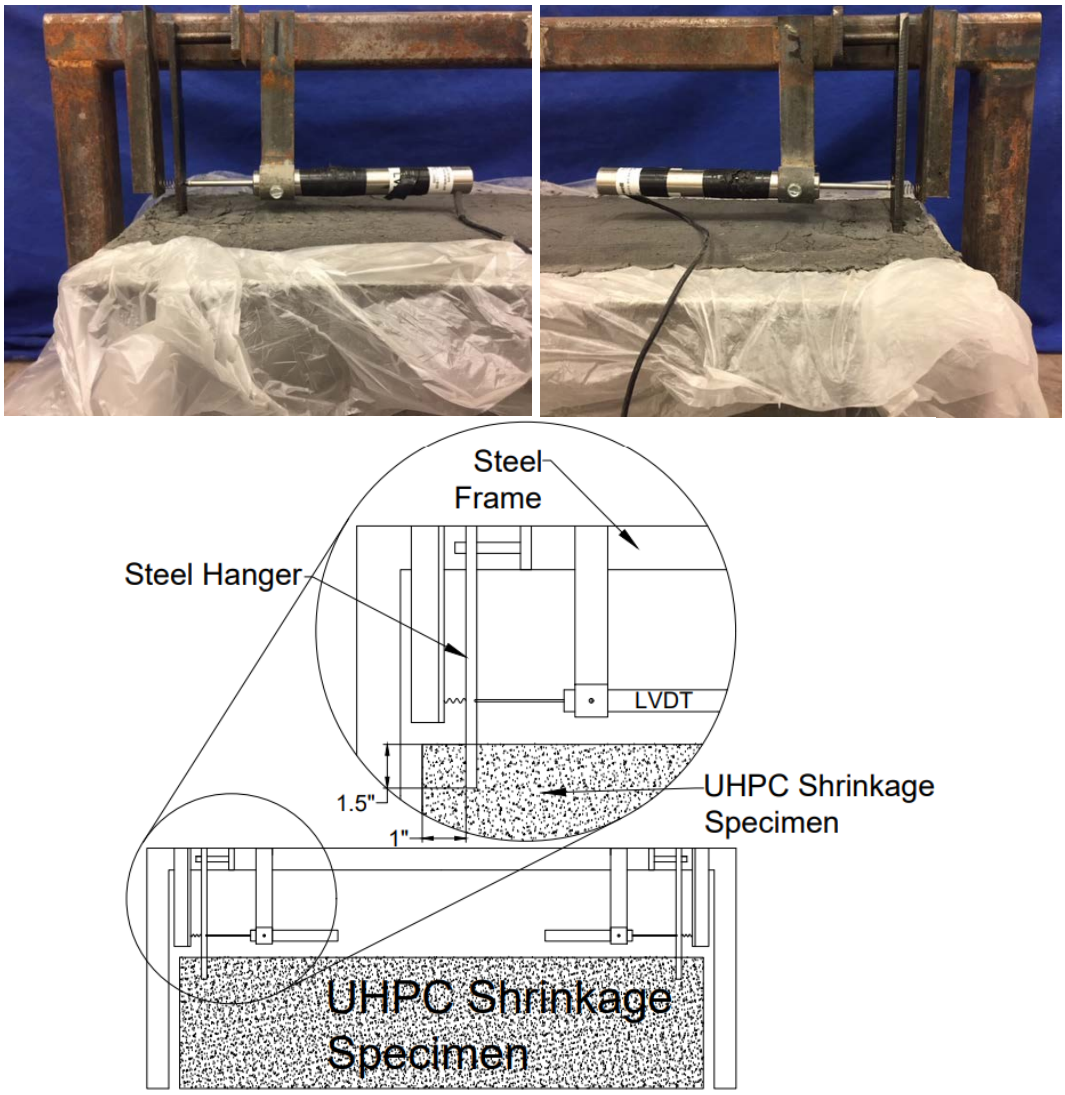

Figure 7. Early-age shrinkage setup.

4.4.2. Longer-Term Shrinkage

Longer-term shrinkage in the grouting material also contributes to shear stresses and direct tension on the bonded interface. Therefore, longer-term shrinkage of UHPC was also characterized.

Longer-Term Shrinkage Setup: Longer-term shrinkage was measured using a modified version of ASTM C157 *(38).* In this modified test, the longer-term shrinkage specimens were 3x4x16 in. (76x102x406 mm) prisms with gage studs (contact points) cast into the ends of the specimens. After curing in the mold for 24 hours, the longer-term UHPC shrinkage specimens were cured in a moist room (73°F [23°C] and 98% relative humidity) for six days. On the seventh day, the specimens were placed in ambient conditions (68°F [20°C] and 30% relative humidity) for the remainder of the shrinkage monitoring. The relative humidity of 30% provided a harsher environment for shrinkage than the 50% relative humidity environment specified in ASTM C157.

For comparison with the wet cured specimens, ambient cured specimens were produced. These specimens were cured at ambient lab conditions for the entire length of the shrinkage monitoring period.

Longer-Term Shrinkage Test: Shrinkage monitoring began immediately after the beams were removed from the molds. Changes in length were measured using a comparator as shown in Figure 8. Measurements were recorded for 28 days that included the seven days of moist curing (73°F [23°C] and 98% relative humidity) and the remaining time at ambient conditions (68°F [20°C] and 30% relative humidity). Specimens cured at ambient lab conditions had measurements recorded for 28 days after demolding. Shrinkage strains for the longer-term shrinkage tests were computed using the changes in length from the comparator readings and Equation 3.

Figure 8. Longer-term shrinkage test setup.

4.5. Full-Scale Channel Girder Tests

Longitudinal four-point flexural testing of two reinforced concrete channel girders connected by a grouted shear key was performed in the Structural Systems and Material Testing Laboratory (SSMTL) at NMSU, as shown in Figure 9. The channel girders were recovered from Bridge 5296, an in-service bridge located 0.7 miles (1.13 km) East of the NM-28 junction in Anthony, NM. Bridge 5296 was a structurally deficient bridge that was recently replaced with Bridge 9706, the first UHPC bridge in New Mexico. Bridge 5296 was constructed with 3 ft. (0.914 m) wide reinforced concrete channel girders with a maximum span length of 25 ft. (7.62 m). The girder cross-section is shown in Figure 10. The reclaimed girders, while having been in-service, were deemed adequate for laboratory testing. Two girders were used to conduct three tests. The first and third tests used locally developed UHPC to grout the shear key. However, the first shear key was cast with no surface preparation of the shear key to improve bond between the girders and the UHPC (referred to as improperly bonded). US Spec NA non-shrink grout, an approved non-shrink grout for use in New Mexico Department of Transportation (NMDOT) projects, was used for the shear key in the second test. Cyclic loading (1000 cycles at service load conditions) was conducted with for the two-girder shear key tests. Additionally, an individual girder was tested to quantify

the load-deflection behavior of a single girder. The final test investigated the overloaded (i.e., post-yield) behavior of the system when the shear key was grouted with UHPC. The test set-up, instrumentation and grouting methods are described in the following sections.

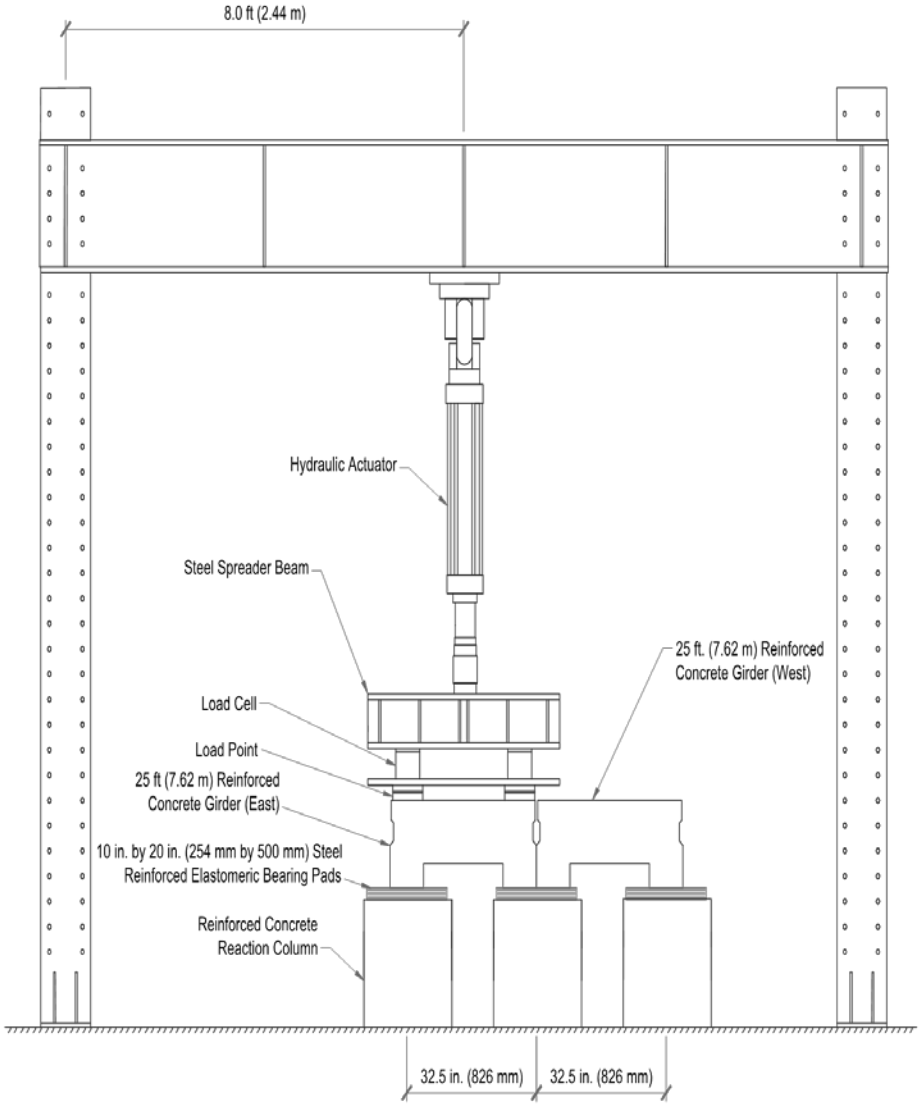

Figure 9. Test set-up for full-scale laboratory testing.

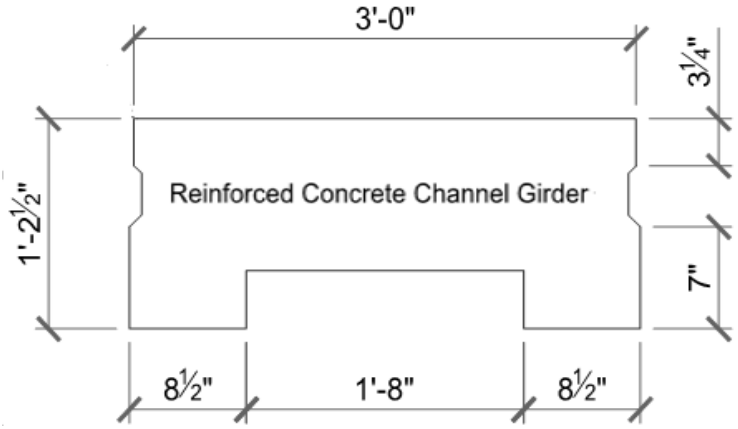

Figure 10. Reinforced concrete channel girder.

4.5.1. Test Setup and Instrumentation

Two reinforced concrete girders were placed adjacently on six short reinforced concrete columns and positioned beneath two, 110-kip (490-kN) capacity hydraulic actuators as shown in Figure 11. Each column had a 2 in. (50.8 mm) steel reinforced elastomeric bearing pad to support the stems of the channel girders.

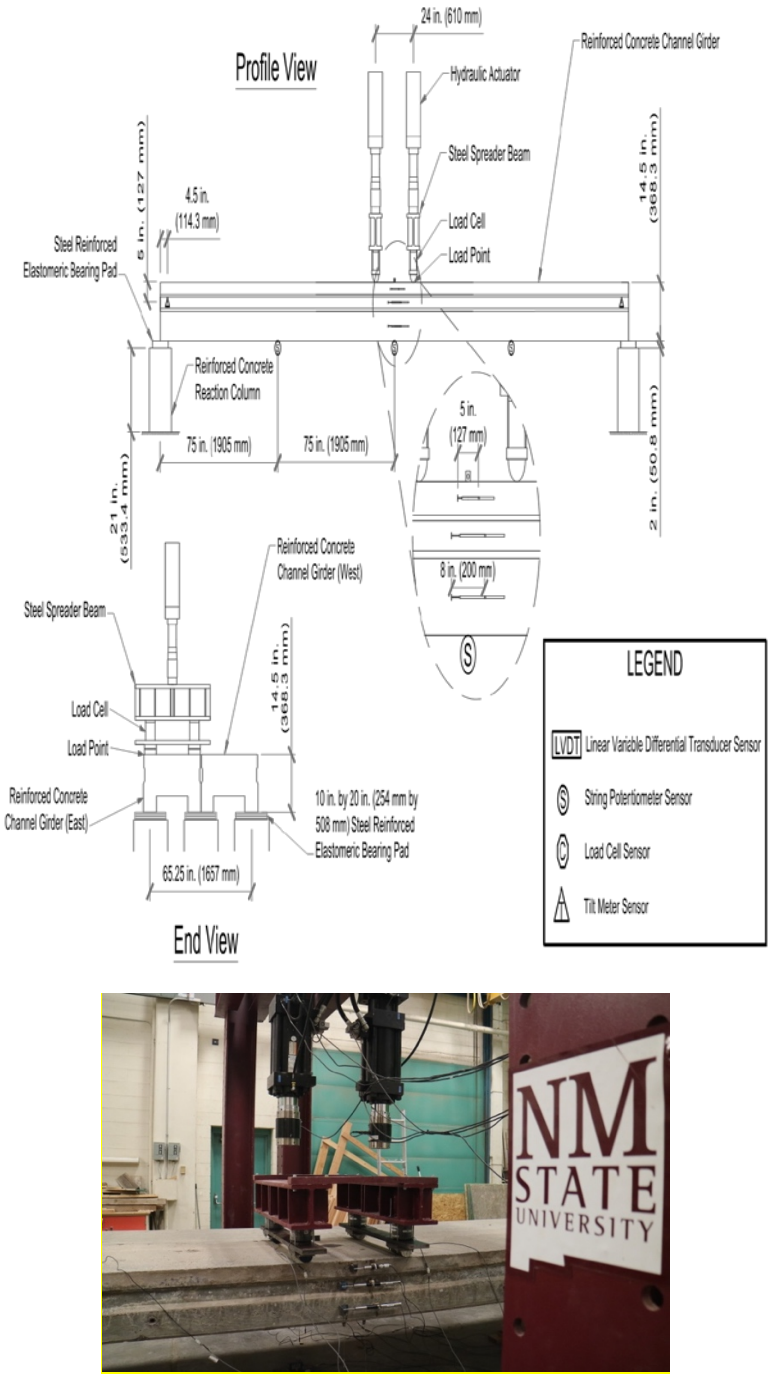

Figure 11. Test setup and instrumentation (a) profile and section view, (b) instrumentation of east girder.

The hydraulic actuators were placed 24 in. (610 mm) apart, each 12 in. (305 mm) from mid-span, to create a nearly pure moment region. Load was applied by setting the actuator displacement to cyclic or monotonic loading using the computer software. During controlled displacements of the actuators, the loads were measured using internal load cells in the actuator heads. As shown in Figure 11, load was distributed using steel spreader beams to 3.0 in. (75 mm) diameter semi-circular load points centered over each stem of the east girder to create a four-point loading

configuration. The load at each point was recorded with additional load cells to capture distribution of loading.

The girder was instrumented with multiple sensors to measure the behavioral response of both girders to flexural loading (Figure 11 and Figure 12) and determine the efficiency of shear and moment transfer across the shear key. Electronic clinometers, also known as tiltmeters, were placed at mid-depth of the exterior face of each girder over each support to record girder rotation and measure the symmetry of the applied loads. String potentiometers were attached to the bottom of the interior stems at quarter points and at mid-span to measure vertical deflections of the girder. Two additional string potentiometers were placed at mid-span on the bottom of the east exterior stem.

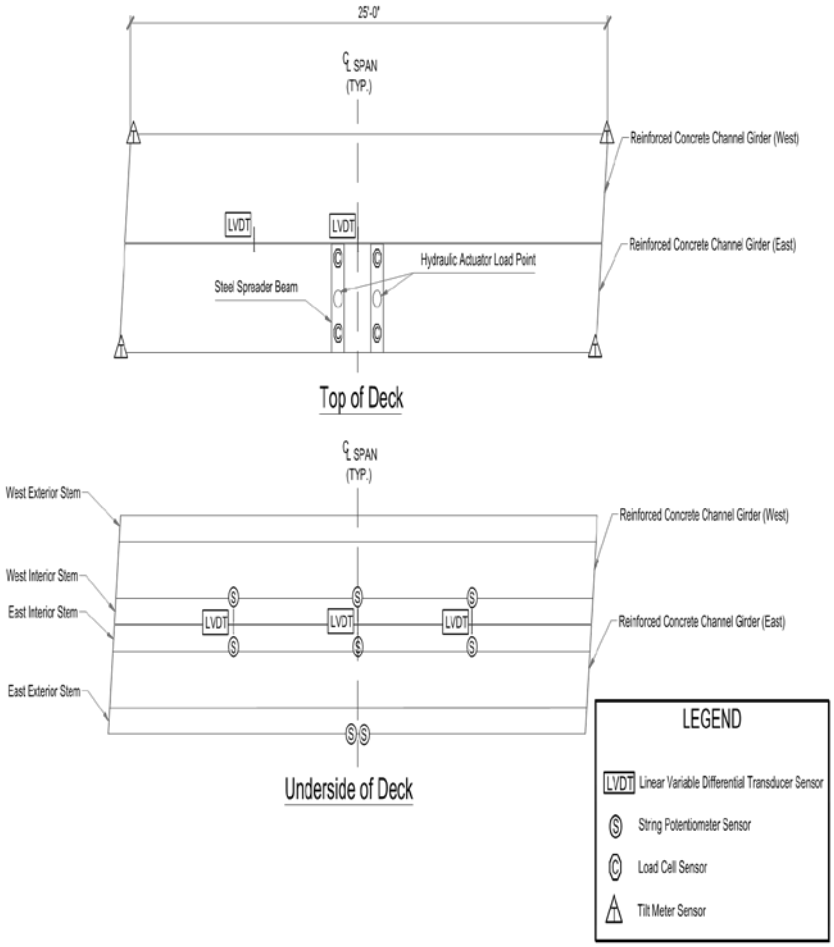

Figure 12. Test setup and instrumentation plan view.

LVDT's were used to measure axial displacements in the girders near mid-span, which were then used to calculate curvature of the girders. To accomplish this, three LVDT's were placed at different elevations on the exposed longitudinal face of each girder at mid-span as shown in the oval detail provided in Figure 11. To record any gap openings in the shear key, LVDT's were also placed across both the top and bottom of the shear key joint at one quarter point and at mid-span as shown in Figure 12. All sensors were connected to a data acquisition system, facilitating real time monitoring and data collection throughout testing.

4.5.2. Grouting Mixtures

UHPC and US Spec NA non-shrink grouts were used as the grouting materials for these tests. The UHPC grout used the same mixture proportions described in section 4.1 of this report. Mixing was performed with a vertical pan mixer. The US Spec NA non-shrink grout is an NMDOT approved non-shrink grout product. The non-shrink grout mixture proportions are presented in Table 3. When mixing, adequate workability of the non-shrink grout was achieved with 9.2% less water than stated as the maximum recommended water content by the manufacturer. The weight of water used is provided in Table 3.

Table 3. US Spec NA non-shrink grout mixture proportions.

Materials	Cement	Silica Fume	Fly Ash	Crystalline Silica	Water
%	40 - 80	5 - 20	5 - 20	>0.1	-
lb/yd^3 (kg/m^3)	1020-2040 (608-1217)	128-510 (76-304)	128-510 (76-304)	>2.55 (1.52)	750 (448)

During casting of each of the three shear keys, 4 in. (101.6 mm) cubes, a 4 in. by 8 in. (101.6 mm by 203.2 mm) cylinder and a 6 in. by 12 in. (152.4 mm by 304.8 mm) cylinder were cast for compressive strength testing and modulus of elasticity measurements.

4.5.3. Grouting Methods

Before casting of the shear keys, the bottom of the shear key joint was sealed with caulk to ensure that all grout remained in place until the grout had set. To produce the improperly bonded UHPC shear key, the walls of the shear key were neither saturated with water nor intentionally roughened. By not preparing the walls of the shear key, the expectation was that the UHPC would not be able to create an effective bond with the precast concrete girder. Casting of the UHPC grout was performed by placing the grout through the longitudinal gap located on the top of the shear key. To facilitate the consolidation of UHPC in the shear key, a pencil vibrator with a diameter of 0.25 in. (6.35 mm) was used during placement. After casting, plastic was placed over the shear key to decrease evaporation and facilitate strength gain of the UHPC. The plastic remained on the shear key for 24 hours, and then the shear key was covered in wet burlap for the duration of curing.

Prior to casting the US Spec NA non-shrink grout, the walls of the shear key were wetted to produce a more effective bond. When mixing the non-shrink grout, the workability was reached with 9.2% less water than stated as the maximum water content recommended by the manufacturer. Casting was performed by pouring the grout into the top of the shear key. No vibration was required due to the flowable state of the grout. Upon completion of casting, the shear key was covered with plastic to prevent loss of moisture and aid strength gain. After 24 hours, the plastic was removed, and the shear key was covered with wet burlap to maintain wet curing conditions.

For casting of the fully bonded UHPC shear key, the walls of the key were wetted to assist bond between the UHPC and precast concrete. The UHPC was then placed in the top of the shear keyway and vibrated using the pencil vibrator. Plastic was placed over the top of the shear key to prevent moisture loss. After 24 hours, the plastic was replaced with wet burlap to provide constant moisture for an effective cure.

4.5.4. Cyclic Loading

Deflection Criteria for Cyclic Loading: Deflection limits from the AASHTO LRFD Bridge Design Specifications *(39)* are summarized in Table 4. These deflection limits include:

1. Criteria for deflections as outlined by AASHTO 2.5.2.6.*2 (39*). The criterion selected states an allowable deflection limit for general vehicular loads on concrete bridges equal to Span/800. For the clear span of 288 in. (7315 mm) used for testing, the allowable deflection limit was calculated to be 0.360 in. (9.14 mm).

2. Application of design truck as outlined by AASHTO 3.6.1.2.2 *(39)*. Characteristics of the design truck are provided in Figure 13. The 72-in. (1830 mm) transverse spacing of wheels allows only a single wheel load from each axle to be present on the 36 in. (914 mm) width of one reinforced concrete channel girder. Thus, a distribution factor of one (DF = 1.0) was conservatively assumed for the following two configurations:

    a. To produce the most extreme force effect, the 32.0-kip (142-kN) axles were assumed to be spaced at 14.0 ft. (4.27 m), with one 16-kip (71.2-kN) wheel load from each of the two axles placed on the girder equidistant from mid-span. The mid-span deflection due to this configuration was calculated to be 0.228 in. (5.80 mm).

    b. The total force of a single 32.0-kip (142-kN) axle was assumed to act as a point load at mid-span. The mid-span deflection due to this configuration was calculated to be 0.388 in. (9.85 mm).

Table 4. Summary of deflection criteria for cyclic loading.

Case	Load	Criterion	Description	Deflection in. (mm)
1	Span/800	AASHTO 2.5.2.6.2	Girder clear span of 288 in. (7315 mm)	0.36 (9.14)
2a	Design Truck	AASHTO 3.6.1.2.2	16.0-kip (71.2-kN) axles spaced 14.0 ft. (4.27 m) and positioned equidistant from girder mid-span	0.23 (5.79)
2b	Design Truck	AASHTO 3.6.1.2.2	32.0-kip (142-kN) point load at girder mid-span	0.39 (9.86)
			Cyclic Loading Target Deflection	0.4 (10.16)

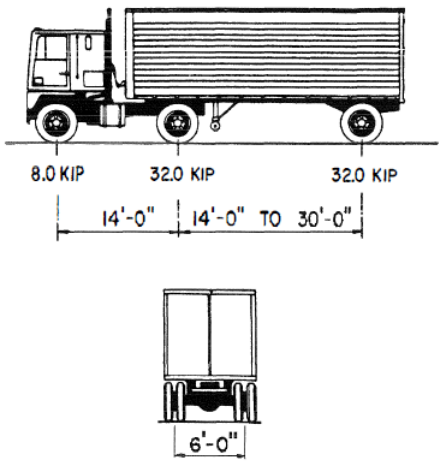

Figure 13. Characteristics of the design truck *(39)*.

Cyclic Testing: The first full scale test conducted was cyclic loading of the reinforced concrete channel girders with the shear key grouted with improperly bonded UHPC, herein referred to as Cyclic Loading 1 (CL1). Using the loading configuration shown in Figure 11, the girder was first loaded at a constant rate 0.05 in./min (1.27 mm/min) to a mid-span deflection target of 0.40 in. (10.2 mm). Once the required actuator displacement was reached, the girder was unloaded, and the loading was repeated for a total of 1000 load-unload cycles. The loading rate was set at 2 cycles/min for the first 50 cycles, before being increased to 4 cycles/min for the remaining 950 cycles.

After completing CL1, the girders were separated and the UHPC grout was removed. The girders were then repositioned and prepared for the second test, which included wetting the shear key walls to ensure a more efficient bond with the grouting material. The second test used US Spec NA non-shrink grout as the shear key grouting material. The same testing set up and loading sequence used for CL1 were used for this test to facilitate comparison of results. This test is referred to as Cyclic Loading 2 (CL2).

Upon completion of CL2, the girders were once again separated, and the grouting material was removed. At this point, a single girder was subjected to cyclic loading to quantify the behavior of the girder when no adjacent girder was available for load transfer. For this test, the east girder was instrumented as described in Figure 14. To remain consistent, cyclic loading of the single girder, herein referred to as Cyclic Loading 3 (CL3), was performed by loading the girder at a constant rate of 0.05 in/min (1.27 mm/min) to the desired deflection of 0.40 in. (10.2 mm) and then unloading. A total of three load-unload cycles were completed.

For the final full-scale test, the girders were once again placed adjacently, and the shear key wetted to assist bonding of the UHPC grout. This test, referred to as Cyclic Loading 4 (CL4), used the same test set up described for CL1 and CL2 and shown in Figure 11. The girders were loaded to the desired deflection at a constant rate of 0.05 in/min (1.27 mm/min), unloaded, and then cycled for 100 load-unload cycles at 2 cycles/min. After completion of the 100 cycles, the deflection was increased to ultimate loading.

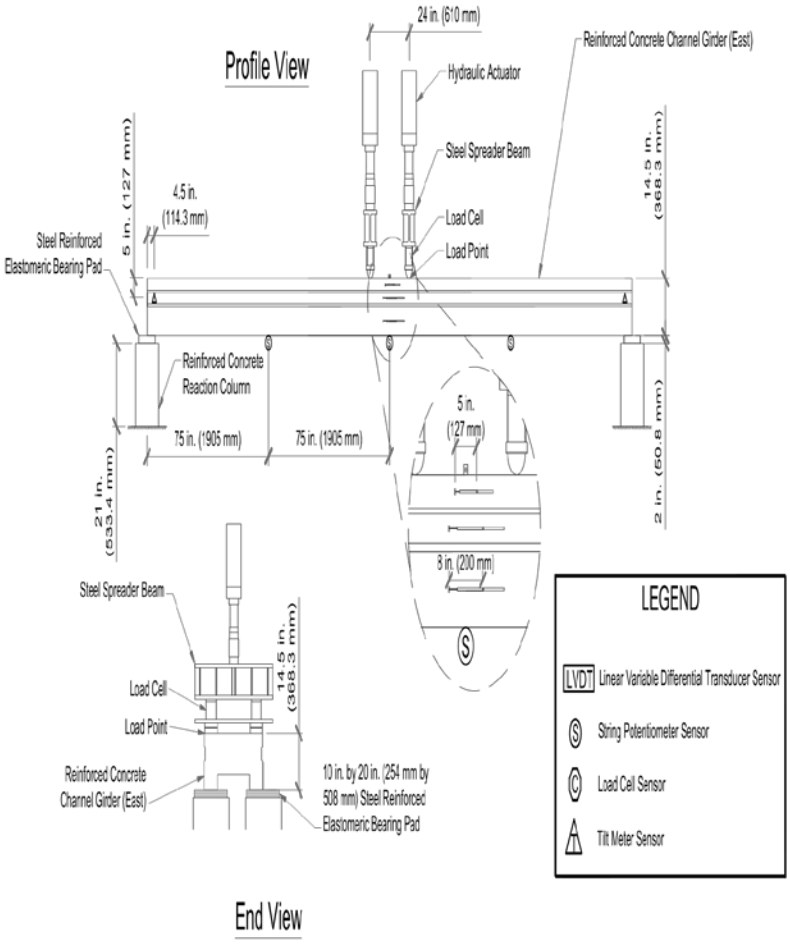

Figure 14. Test setup and instrumentation profile and section view of single girder.

4.5.5. Ultimate Loading

Ultimate loading of the reinforced concrete channel girders was performed with longitudinal four-point bending as shown in Figure 11. The girder was loaded again to the service displacement of 0.40 in. (10.2 mm), from which loading was increased to a deflection of 0.8 in. (20.3 mm). The girder was then unloaded to the initial 0.40 in. (10.2 mm) of deflection. This process continued with an increase in maximum deflection of 0.40 in. (10.2 mm) after every unload cycle until a maximum deflection of 2.0 in. (50.8 mm) was reached. At this point, the girders were cycled between 0.40 in. (10.2 mm) and 2.0 in. (50.8 mm) of deflection for three cycles at a constant rate of 0.1 in/min (2.54 mm/min). At the completion of these cycles, the girders were unloaded, and the residual deflection was measured. To complete the test, the girders were loaded to 0.40 in. (10.2) of deflection, accounting for residual effects, and cycled for another 100 load-unload cycles at a rate of 4 cycles/min.

5. ANALYSIS AND FINDINGS

5.1. Compressive Strength

Table 5 presents the average compressive strengths obtained from 3.94 in. (100 mm) cube specimens for the UHPC and 6x12 in. (152x305mm) cylinder specimens for the normal concrete used in the bond strength tests. The minimum 28-day strength required for UHPC, according to ASTM C1856, is 17,000 psi (120 MPa) *(8).* The UHPC mixture used in this research met that requirement. The 28-day compressive strength for the normal strength concrete was obtained from specimens that were moist cured (73°F [23°C] and 98% relative humidity) to an age of seven days and then cured at ambient conditions (68°F [20°C] and 30% relative humidity) to an age of 28 days. This curing regimen was adopted for the normal strength concrete to match the substrate curing method used for the bond strength tests.

Table 5. Compressive strength results for UHPC and Normal Concrete.

Strength	UHPC 7 day	UHPC 28 day	Normal Concrete 7 day	Normal Concrete 28 day
psi (MPa)	15,690 (108.2)	18,460 (127.3)	2670 (18.4)	3280 (22.6)

5.2. Bond Strength

5.2.1. Slant-Shear

Figure 15 and Table 6 present the average bond strengths from the slant-shear tests conducted at seven and 28 days after UHPC was applied to the substrate. The American Concrete Institute (ACI) recommends a bond shear strength for slant shear of 1000 psi (6.90 MPa) for seven days and 2000 psi (13.8 MPa) for 28 days *(24).* The data shows that each surface texture provided adequate bond at seven days. It was also observed that shear strength increased from seven to 28 days, except for the formed surface where it decreased slightly. Several of the shear strengths at 28 days did not meet the ACI's recommended shear strength of 2000 psi (13.8 MPa). This is attributed to the low strength of the substrate concrete, which may have also have been compromised by cracks caused by chipping during surface preparation. All of the slant-shear fractures with texture occurred in the substrate. However, the substrate was air-entrained, only wet-cured for seven days, and was tested at 28 days. It appears that the strength at 28 days wasn't adequate for the supporting 2000 psi (13.8 MPa) shear strengths.

The low strengths from formed surfaces tested at 28 days appear to be due to variation of the test results within the small population of specimens. However, it is also possible that shrinkage of the UHPC caused some dimensional incompatibility with the substrate that caused a slight loss of bond strength between seven and 28 days.

Table 6. Slant-shear bond strengths.

Texture in [mm]	7 Day Shear Stress psi (MPa)	28 Day Shear Stress psi (MPa)	7 Day Normal Stress psi (MPa)	28 Day Normal Stress psi (MPa)
Formed	1278 (8.81)	1042 (7.18)	2943 (20.3)	2416 (16.7)
0.0276 [0.71]	1711 (11.8)	2126 (14.7)	3950 (27.2)	4910 (33.9)
0.06 [1.52]	1045 (7.2)	1408 (9.7)	2857 (19.7)	3283 (22.6)
0.13 [3.30]	1368 (9.43)	1549 (10.7)	3215 (22.2)	3580 (24.7)

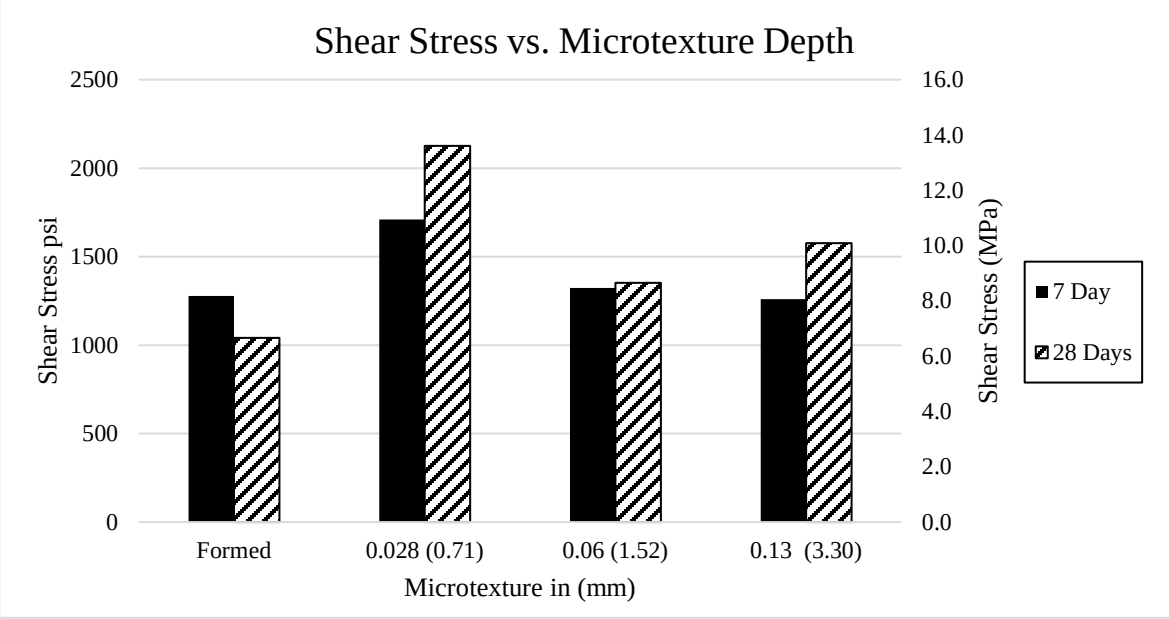

Figure 15. Slant-shear bond strengths.

5.2.2. Direct Tension

Figure 16 and Table 7 present the results from the direct tension tests conducted seven and 28 day after the UHPC was applied to the substrate. ACI recommends a tensile strength for repair concrete at seven and 28 days of 150 psi (1 MPa) and 250 psi (1.72 MPa), respectively *(24).* As shown in Table 7, the strength recommendations were met for the seven-day tests but not for the 28-day tests.

At 28 days, the formed surfaces experienced bond failures that indicate that the bond strength was inadequate. Additionally, the 28-day strengths of the formed surfaces were less than the strengths at seven days. This observation is consistent with the similar decrease seen for formed surfaces in the slant-shear results. It appears that shrinkage of the UHPC may be limiting the bond strength development on formed surfaces.

Table 7. Direct tensile strengths.

Texture (in [mm])	7 Day Tensile Strengths psi (MPa)	28 Day Tensile Strengths psi (MPa)
Formed	166 (1.14)	148 (1.02)
0.060 [1.52]	172 (1.18)	193 (1.33)
0.100 [2.54]	170 (1.17)	152 (1.05)

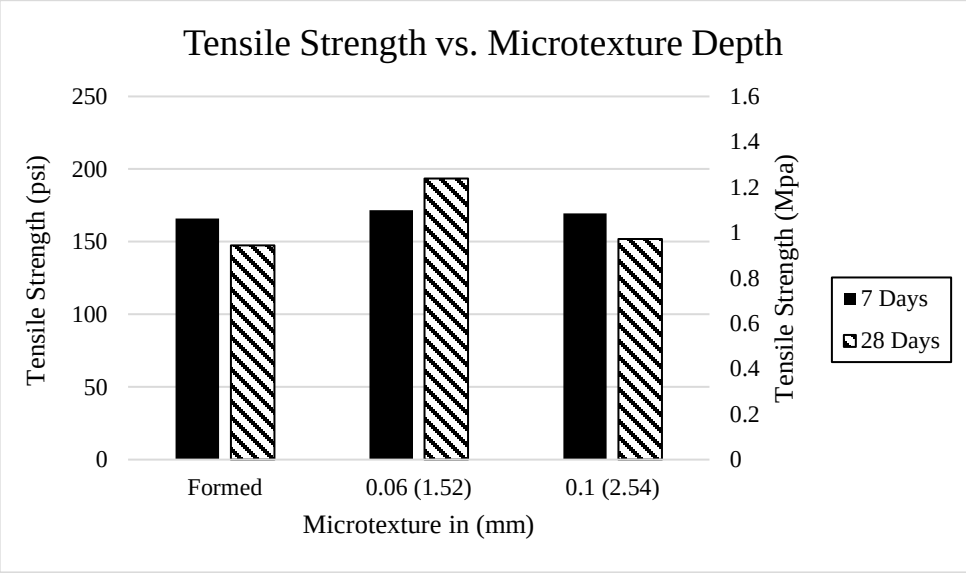

Figure 16. Direct tension strengths.

For the textured surfaces, all of the fractures occurred in the substrate. This is an indication that the bond was excellent, but tensile strength was limited the strength of the substrate. As with the textured slant-shear specimens, substrate strength could also have been reduced by cracks caused by chipping during surface preparation.

5.2.3. Scanning Electron Microscopy

Images were collected for both formed and chipped surfaces of bond strength specimens to provide a visual explanation of the microstructure of fractured bond surfaces. The images in Figure 17 show fly ash residue that remained on the substrate after a bond failure. This indicates that the SCM's produce the majority of the bond. The second image in Figure 17 shows steel fibers protruding from the UHPC after it de-bonded from the substrate. This observation could indicate that the steel fibers might obstruct some of the bond or that some of the fibers are not participating in the behavior of the UHPC.

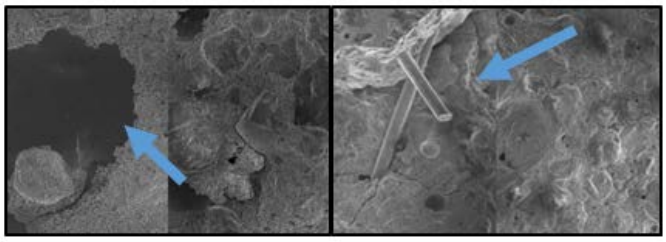

Figure 17. Formed UHPC and normal concrete (left) and textured UHPC and normal concrete (right).

SEM images were also produced from sawn cross-sections to investigate characteristics of intact bonded interfaces. Figure 18 shows a large air void in UHPC, which was observed to have more large air voids throughout the mixture. This was expected since the entrapped air content of the UHPC exceeds 4%. Figure 19 shows a bonded interface between UHPC and the substrate concrete (indicated by the arrows). The SEM image shows that there are no observable defects at the bonded interface.

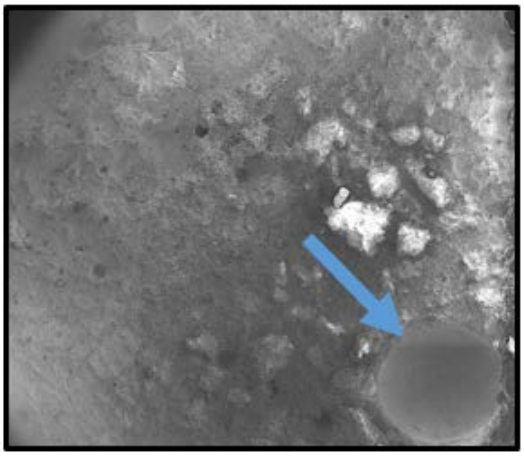

Figure 18. Air voids in the UHPC mixture.

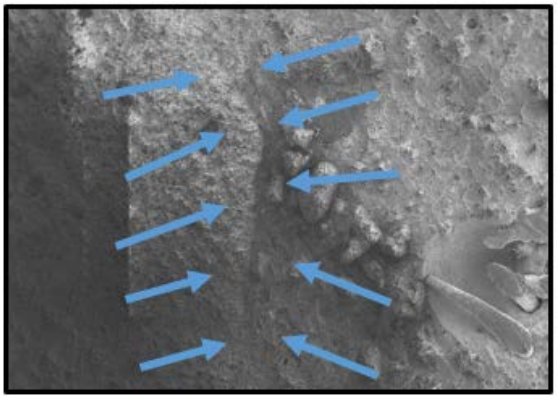

Figure 19. Normal concrete and UHPC interface.

5.3. Shrinkage

5.3.1. Early-Age Shrinkage

The early-age shrinkage tests were conducted on 6x6x24 in. (152x152x610 mm) UHPC beams. Figure 20 presents the early-age shrinkage results from two tests performed for seven days. The total shrinkage strain during this period was approximately 1800 µstrain for Test 1 and 2200 µstrain for Test 2. Figure 21 presents the results from the first 24 hours, during which the total shrinkage strain was approximately 1400 µstrain for Test 1 and 1780 µstrain for Test 2. It is difficult to establish set times for UHPC mixtures because they can be extremely viscous in the fluid state. By stripping molds at early ages and watching for slumped specimens, the set time for the UHPC mixture was estimated to be 10 hours.

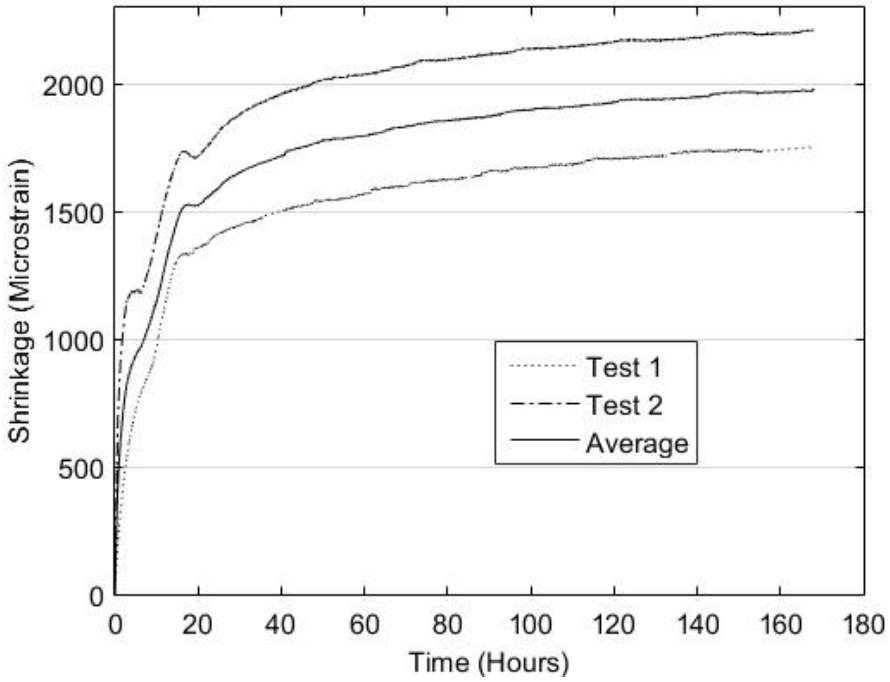

Figure 20. Early-age shrinkage data over seven days.

During the first 10 hours, the UHPC is in a plastic state that may not transfer shear stress to the substrate concrete. Consequently, it appears that although the early-age shrinkage is substantial, approximately 55% (roughly 1000 µstrain) of it occurs in the plastic state and may not contribute to bond stresses since the elastic modulus of the UHPC should be small at such early ages.

Figure 21 shows that Test 2 had a steep slope in the first three hours of testing, which is when Specimen 2 experienced greater shrinkage than Specimen 1. Shrinkage that occurs during the first three hours is not expected to contribute to bond stresses. The shrinkage of Specimen 2 matches well with the shrinkage of Specimen 1 after the first plateau.

Similar early-age shrinkage tests conducted by *(12)* produced the results shown in Figure 22. The magnitude of the shrinkage strains at 24 hours are comparable to those observed in this study.

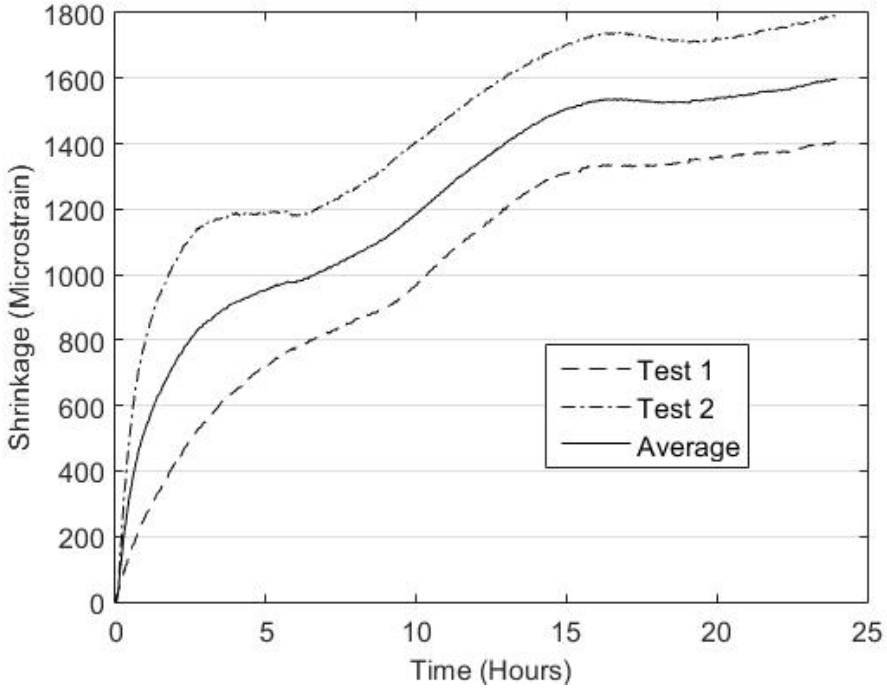

Figure 21. First 24 hours of early-age shrinkage data.

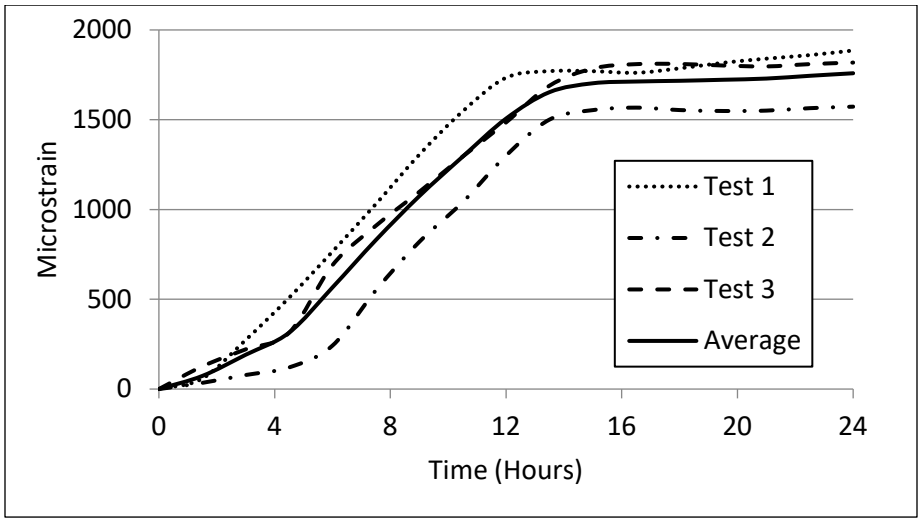

Figure 22. Early-age shrinkage results *(12)*.

5.3.2. Longer-Term Shrinkage

The longer-term shrinkage testing was conducted on 3x4x16 in. (76x102x406 mm) UHPC prisms. Tests were conducted for 28 days by monitoring length changes with a comparator once a day.

Figure 23 presents the results of the longer-term shrinkage tests. The specimens were cured for six days in the moist room (73°F [23°C] and 98% relative humidity) then removed and cured at ambient conditions (68°F [20°C] and 30% relative humidity) for the remainder of the test. This curing method was implemented in Test 1 and repeated in Test 2. For comparison with the wet cured specimens (W), ambient cured specimens (D) were produced and tested in Test 2. As seen in the top plot, shrinkage plateaued around 4 days for both Test 1 and Test 2. Once the specimens

were removed from the moist room on day 7, shrinkage began to increase at a faster rate for both Test 1 and Test 2. Shrinkage began to plateau again around 20 days, at approximately 450 microstrain for Test 1 and 420 microstrain for Test 2. Figure 23 also presents the longer-term shrinkage plot for the ambient cured specimens shown in the bottom plot. Two plateaus occur in this plot as well. The first plateau began on day 5 at around 320 microstrain and the second plateau occurred around day 20 at a shrinkage of approximately 580 microstrain. The ambient cured specimens experienced shrinkage of about 150-170 microstrain greater than the wet cured specimens, which was expected. Figure 24 presents the average longer-term shrinkage data for wet (W) and ambient cured specimens (D) for Test 1 and Test 2.

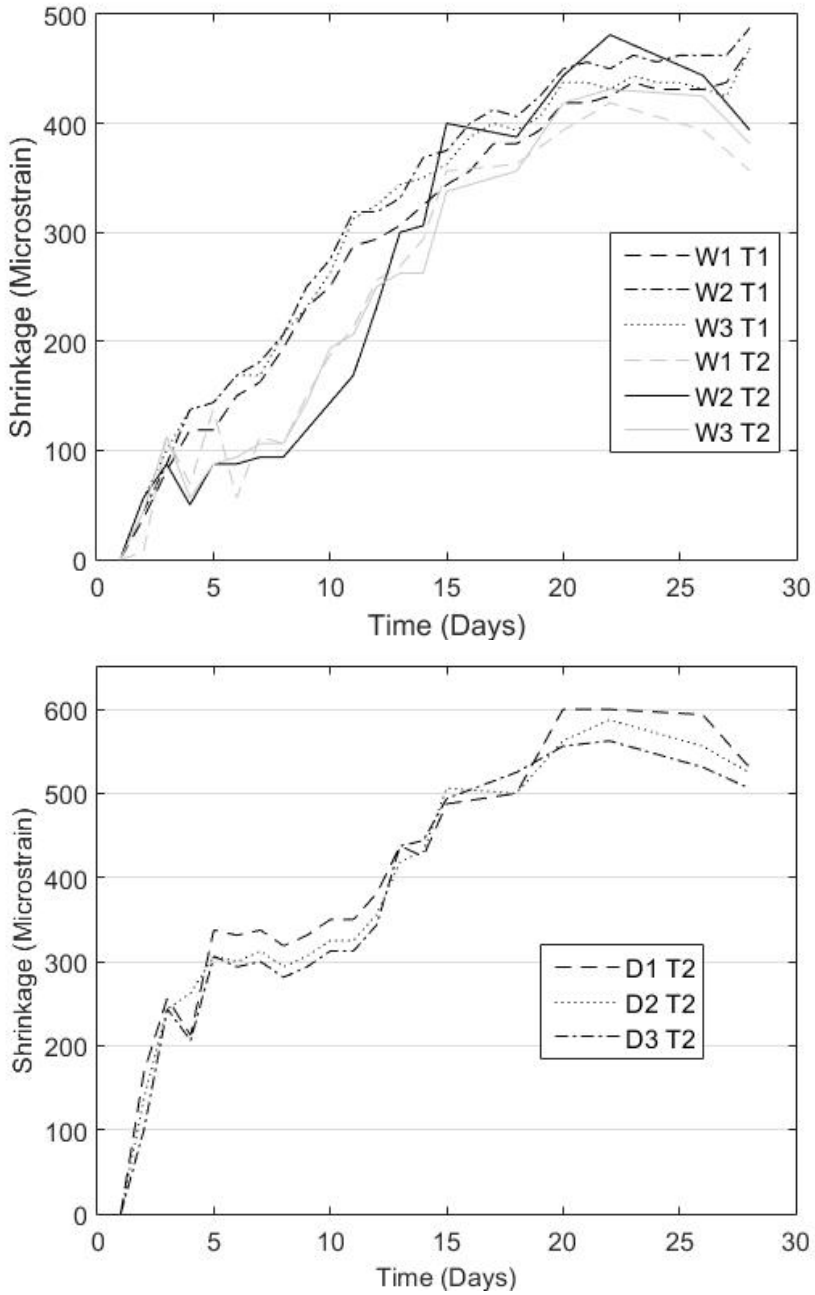

Figure 23. Longer-term shrinkage results, ambient cured (bottom), wet cured (top).

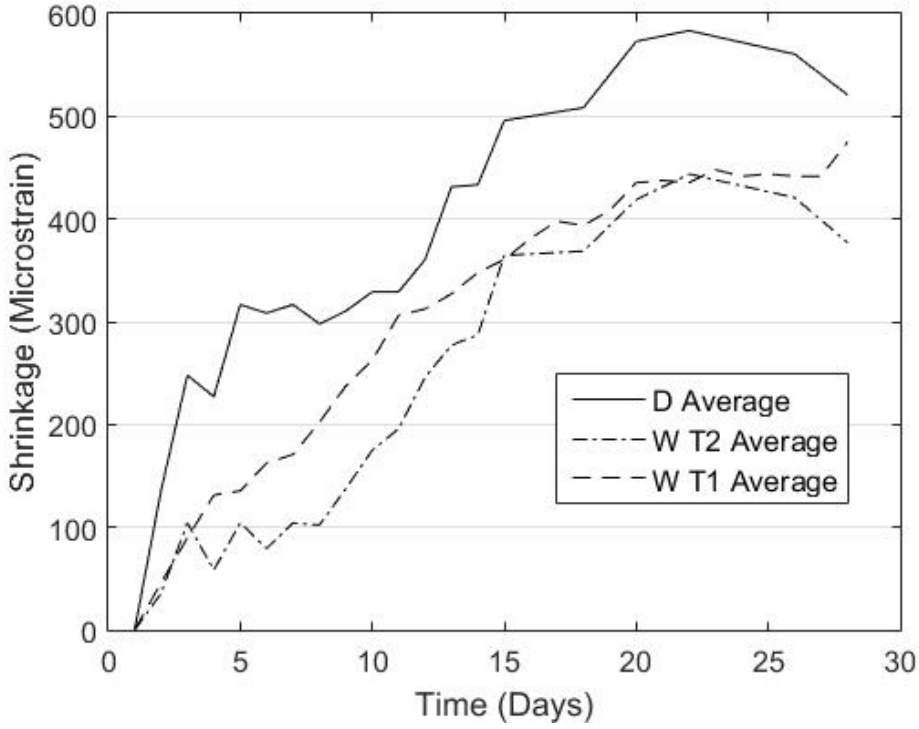

Figure 24. Average longer-term shrinkage results for D and W.

5.4. Full-Scale Channel Girder Tests

5.4.1. Load Deflection Behavior

The full-scale tests were used to assess the load-deflection behavior and shear and moment distribution of the two adjacent girders. Deflections caused by the longitudinal four-point loading, which was applied to a single girder as shown in Figure 11, were used as a measure of the transfer of load through the shear key. Load and deflection were measured with internal load cells located inside the hydraulic actuators and string potentiometers located as discussed in section 4.5 of this report. Load-deflection results were analyzed by plotting load versus the vertical mid-span deflection recorded throughout flexural testing. When analyzing the moment distribution, the mean moments computed from measurements during CL3 were compared with the moments obtained from tests CL1, CL2, and CL4. The sum of both actuator loads was applied when analyzing total load versus deflection and when calculating the total moment of the girders. These load cells have an accuracy of approximately ± 15.0 lb. (66.7 N).

Cyclic Loading 1: The first test performed, CL1, utilized UHPC as the shear key grouting material without preparing the keyway for proper bonding of the grout. Therefore, the UHPC was considered improperly bonded. The assemblage was loaded as shown in Figure 11. The east girder was loaded at a constant mid-span deflection rate of 0.05 in/min (1.27 mm/min) until a mid-span deflection target of 0.40 in. (10.2 mm) was reached, and then cycled through 1000 load-unload cycles.

Figure 25 shows the load-deflection behavior observed between the east and west girders at the string potentiometer locations shown in Figure 12. The greatest difference in deflection between the girders was found to occur at the mid-span locations. For the interior stems, the average difference in deflection between the east and west girders was found to be 0.017 in. (0.43 mm), shown in Figure 25a. The difference in deflection was greatest, however, when comparing the exterior stem of the east girder and the interior stem of the west girder. This difference was found to be 0.084 in. (2.13 mm). These results were expected, considering the lack of support on the east side of the loaded girder compared to the west side where the two girders were joined. The limited difference in deflection between the two interior stems suggests that the girders were deflecting nearly equally, and therefore, transferring load adequately. The average peak load and mid-span deflection throughout CL1 were calculated as 13.9 kips (61.9 kN) and 0.41 in. (10.4 mm), respectively. The girders also appeared to remain linear elastic throughout the duration of test CL1.

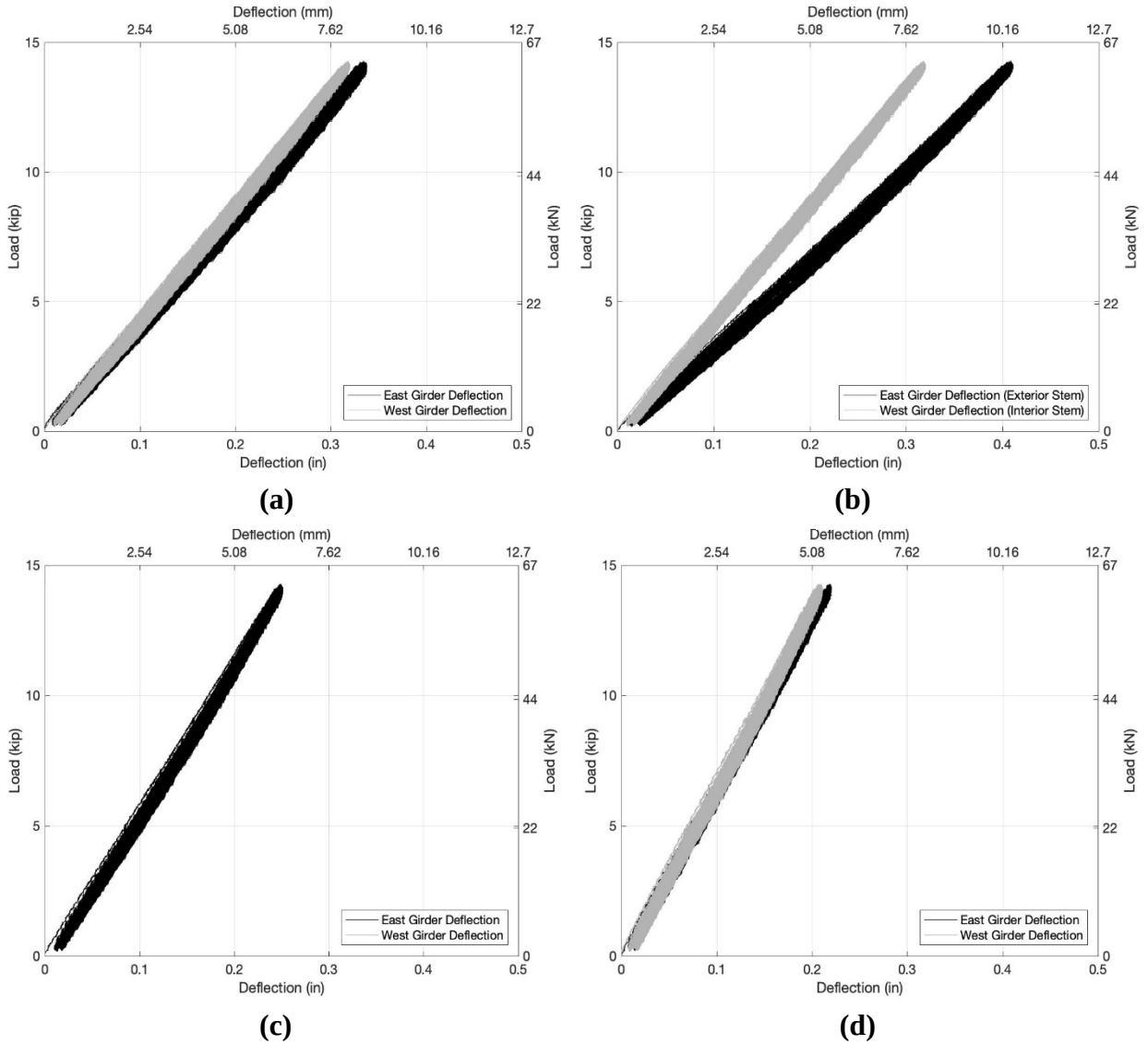

Figure 25. Load versus deflection of east and west adjacent girders for Cyclic Loading 1: (a) interior stems of each girder at mid-span, (b) exterior stem of east girder and interior stem of west girder, (c) interior stems of each girder at first quarter point of span, and (d) interior stems of each girder at third quarter point.

Cyclic Loading 2: The second test used US Spec NA non-shrink grout as the shear key material. This test, referred to as Cyclic Loading 2 (CL2), was performed using the same methodology as CL1 to facilitate comparison of results. The load configuration shown in Figure 11 was used during this test to load the east girder to a mid-span deflection of 0.40 in. (10.2 mm) and then subject it to 1000 load-unload cycles. The load deflection results for CL2 are presented in Figure 26.

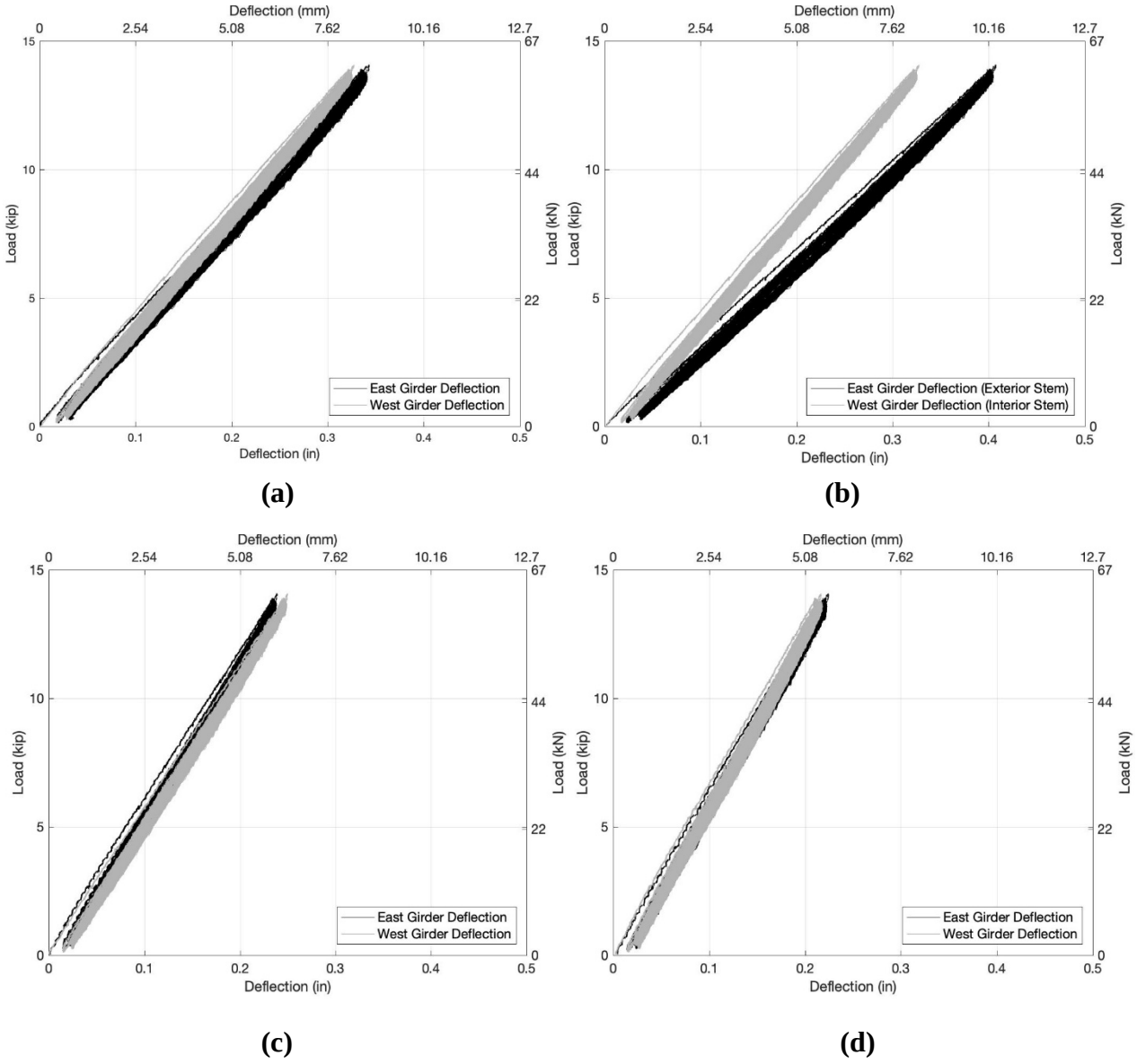

Figure 26. Load versus deflection of east and west adjacent girders for Cyclic Loading 2: (a) interior stems of each girder at mid-span, (b) exterior stem of east girder and interior stem of west girder, (c) interior stems of each girder at first quarter point of span, and (d) interior stems of each girder at third quarter point.

Figure 26 shows the difference in the deflection between the east and west girders at each string potentiometer location shown in Figure 12. As with CL1, the greatest difference in girder deflections was observed at mid-span. This result is due to the high moment region and maximum deflections occurring at mid-span. The average difference in deflection of the two interior stems was found to be 0.015 in. (0.381 mm), shown in Figure 26a. In comparison, Figure 26b shows the

deflection of the exterior stem of the east girder and the deflection of the interior stem of the west girder. The exterior girder and interior girder had a difference in deflection of 0.081 in. (2.06 mm). When comparing the differential deflection of the two girders at mid-span to those measured during CL1 it was found that the differential displacement for CL1 was approximately 0.003 in. (0.08 mm) greater than for CL2. The decreased deflections for CL2 indicate slightly better load transfer across the shear key. This improvement is attributed to improved bond by the non-shrink grout that was likely aided by preparation of the shear key surface.

The east girder for CL2 also had a greater exterior stem deflection compared to the interior stem, due to a lack of support and load transfer. The average peak load applied to the girders in the CL2 test was calculated to be 13.4 kips (59.6 kN), with an average peak mid-span deflection of 0.40 in. (10.2 mm).

Cyclic Loading 3: The next cyclic test completed, CL3, was performed on a single girder with no grouted shear keys. The east girder alone was tested using the instrumentation and four-point longitudinal load configuration shown in Figure 14. The girder was loaded to a mid-span deflection of 0.39 in. (9.91 mm) and then subjected to three load-unload cycles. This test provided measurements of the load-deflection behavior of a single girder.

Figure 27 presents the load-deflection results recorded during CL3. Results from CL3 showed that an average load of 7.40 kips (32.9 kN) was required to induce a deflection of 0.40 in. (10.2 mm). This average is approximately half the recorded load from both the CL1 and CL2 tests. This information was used to calculate the moment distribution factor. During the CL3, test the girder behavior remained linear and no damage was observed.

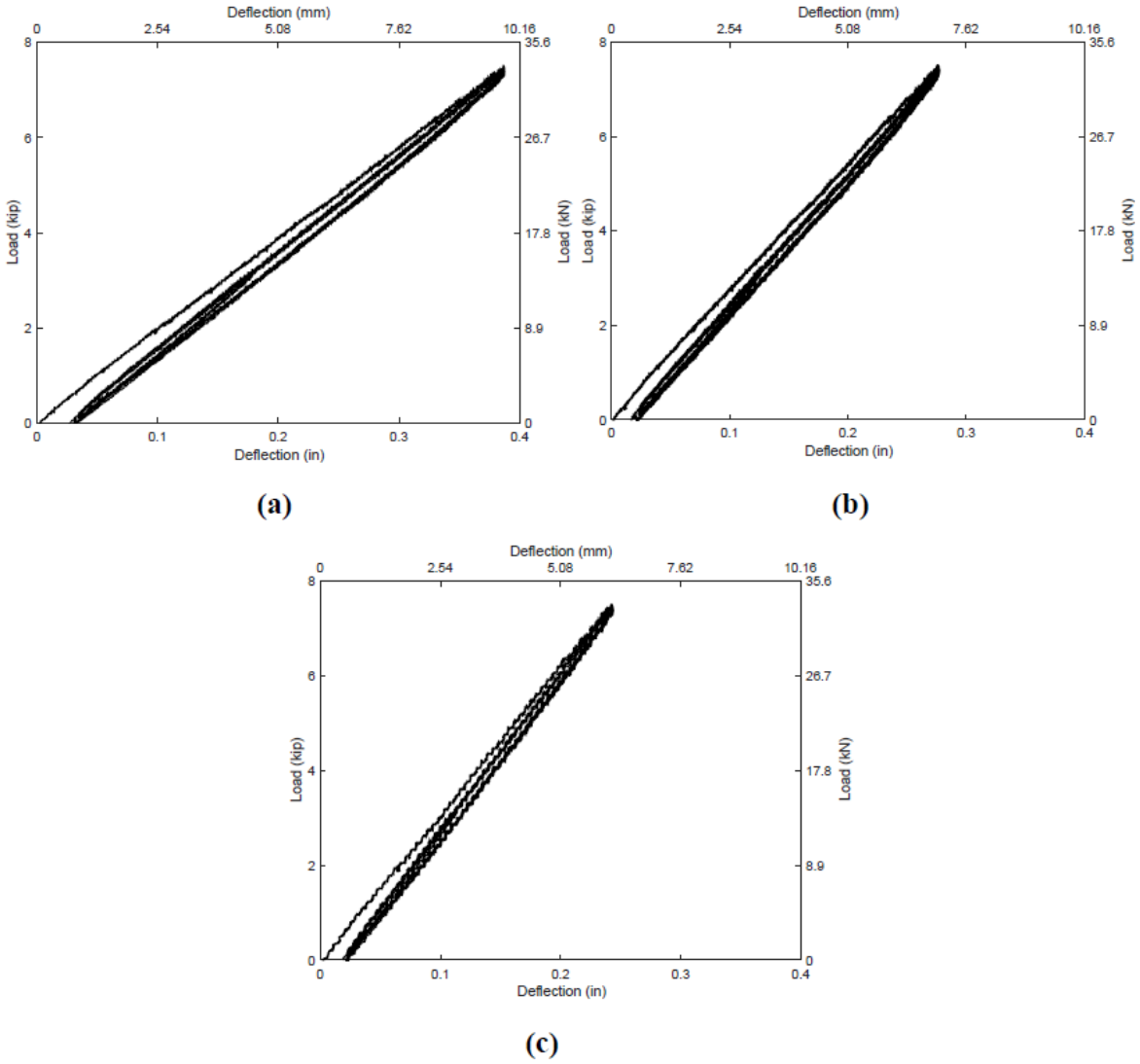

Figure 27. Load versus deflection of east and west adjacent girders for Cyclic Loading 3: (a) mid-span, (b) first quarter point of span, and (c) third quarter point of span.

Cyclic Loading 4: The final full-scale test performed used UHPC as the shear key grouting material. Prior to casting the UHPC shear key, the girder was wetted to ensure a more effective bond between the precast girder and the UHPC material. The Cyclic Loading 4 (CL4) test was performed with the four-point load configuration and instrumentation shown in Figure 11 and Figure 12 The east girder was loaded to a mid-span deflection of 0.4 in. (10.2 mm) and then subjected to 100 load-unload cycles. After completion of cyclic testing the ultimate load testing began.

As shown in Figure 28, the average deflection and load during CL4 were found to be 0.40 in. (10.2 mm) and 13.2 kips (58.7 kN), respectively. The greatest difference in girder deflection continued to occur at mid-span. The differential deflection between interior stems was found to be 0.04 in. (1.02 mm) while the east exterior stem and west interior stem were found to have a difference in deflection of 0.14 in. (3.56 mm). This differential deflection is an increase when compared to tests CL1 and CL2. No cracking or de-bonding was observed during CL4.

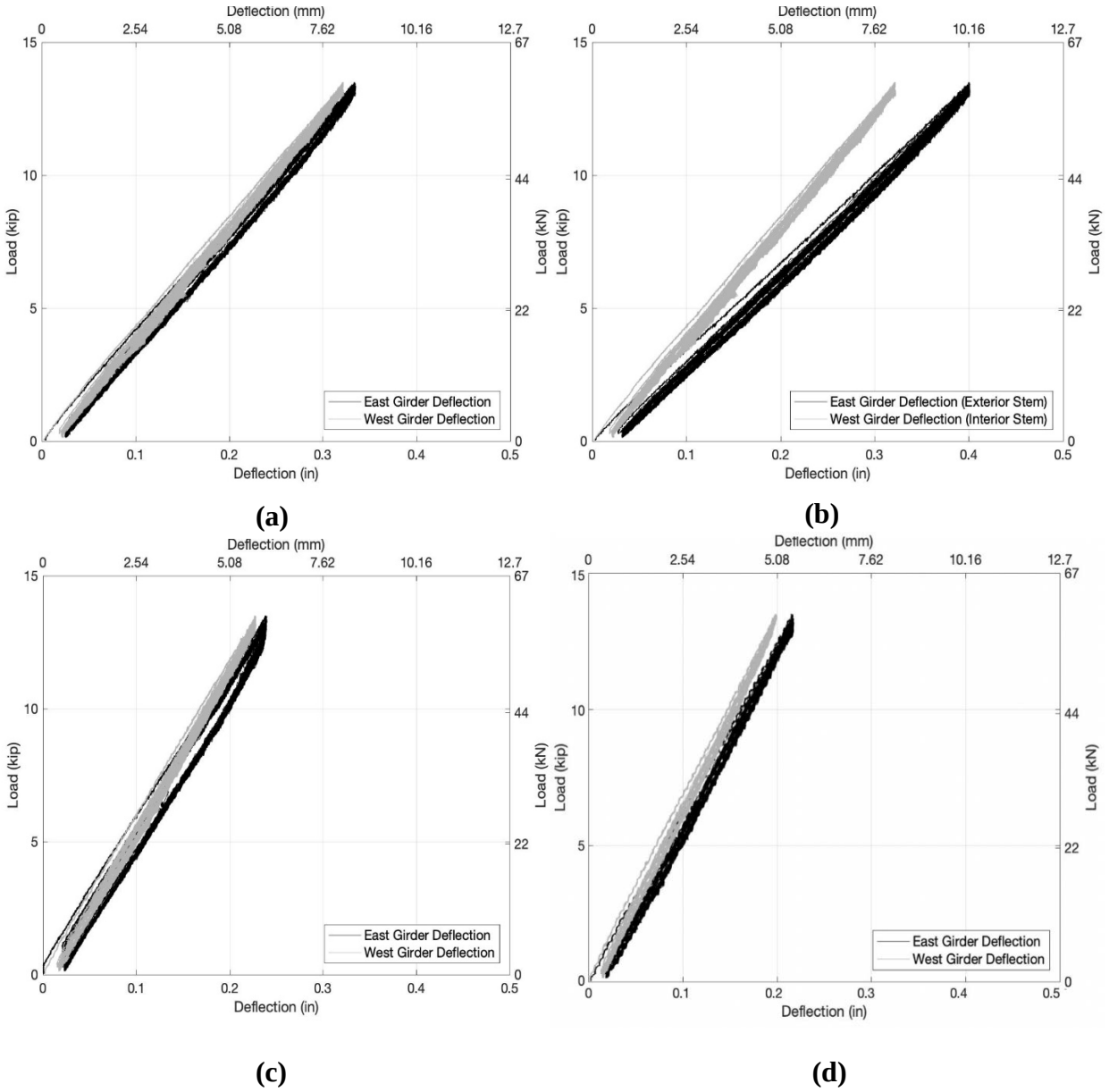

Figure 28. Load versus deflection of east and west adjacent girders for Cyclic Loading 4: interior stems of each girder at mid-span, (b) exterior stem of east girder and interior stem of west girder, (c) interior stems of each girder at first quarter point of span and (d) interior stems of each girder at third quarter point.

5.4.2. Comparison of Cyclic Loading

By comparing the load-deflection behavior across the four cyclic tests, the behavior of each grouting method was analyzed. In Figure 29 the load-deflection response of each mid-span deflection location is graphed. As shown in Figure 29, the stiffness (slope of load-deflection behavior) of the assemblages decreased slightly in the order of testing (stiffest for CL1, least stiff for CL4). The changes in stiffness seem to occur between tests, while the assemblages behave elastically during the individual tests. This could be caused by damage in the girders from being previously in-service and accumulated damage from prior tests. However, the changes are so slight, that it is difficult to place any significance on the observation. As shown in Figure 29, each

stem decreased by approximately the same load capacity indicating that it was the girder or test setup losing stiffness, and not reflective of the shear key performance. The more important observation is that each grouting material behaved similarly, and each two-girder system nearly doubled the load carrying capacity of a single girder. This result implies that there is little mechanical difference between the three shear key designs.

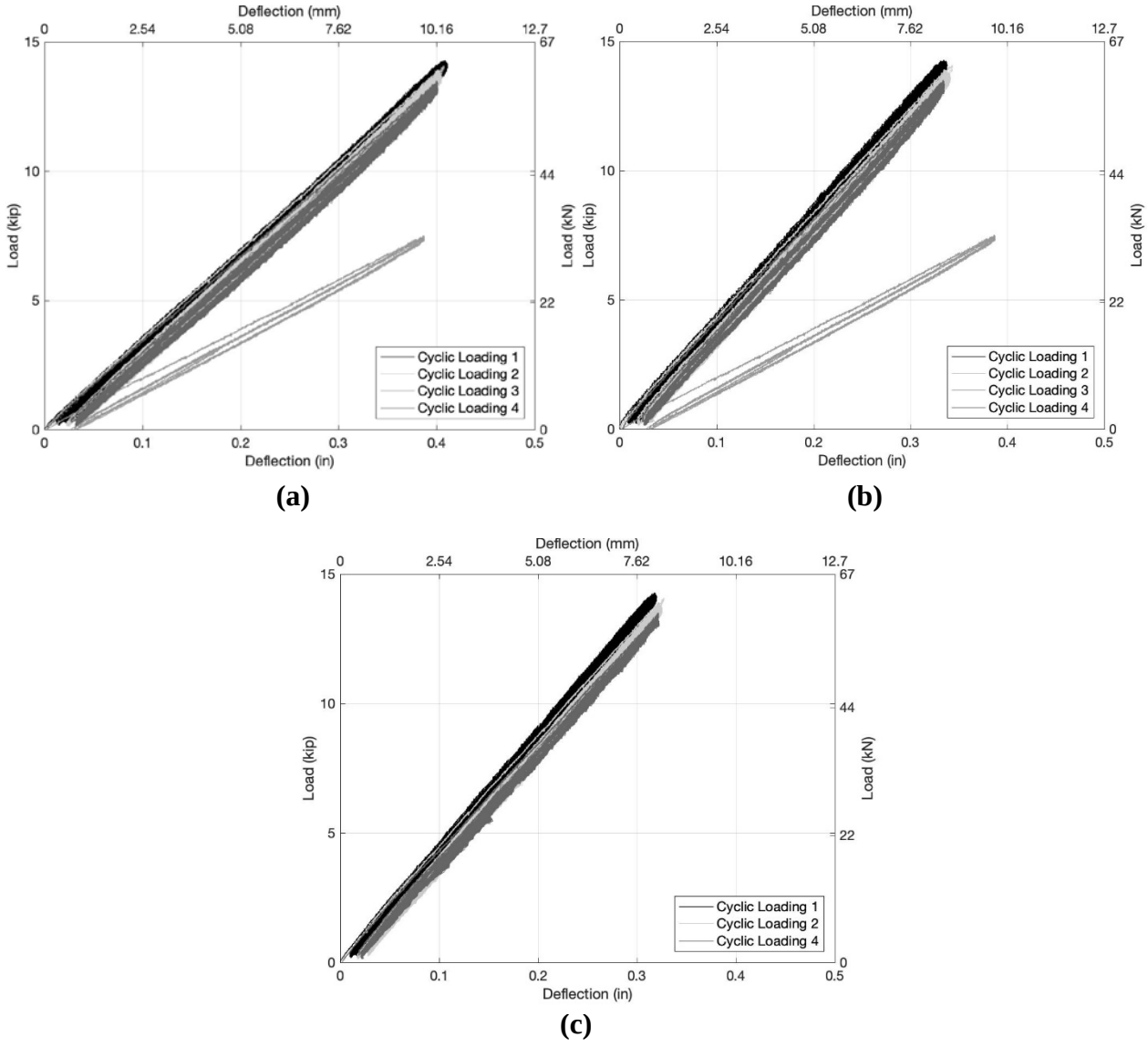

Figure 29. Comparison of load versus mid-span deflection behavior of adjacent girders: (a) exterior stem of east girder, (b) interior stem of the east girder, and (c) interior stem of the west girder.

5.4.3. Ultimate Loading

The final test performed was the ultimate loading of the reinforced concrete channel girder assemblage used in CL4. This test was intended to emulate an overload situation. The ultimate loading of the channel girders was performed with longitudinal four-point bending as shown in Figure 11. Loading began at an initial deflection of 0.40 in. (10.2 mm) and was increased to a deflection of 0.80 in. (20.3 mm). The girder was then unloaded to the previous 0.40 in. (10.2 mm)

of deflection. This process continued with an increase in peak deflection of 0.40 in. (10.2 mm) after every unload cycle until a maximum deflection of 2.0 in. (50.8 mm) was reached. Five times the service displacement, i.e., 2.0 in. (50.8 mm) of deflection, exceeded the AASHTO deflection criteria sufficiently to represent the desired overload behavior. At this point, the girders were cycled between 0.40 in. (10.2 mm) and 2.0 in. (50.8 mm) of deflection for three cycles at a constant rate of 0.1 in/min (2.54 mm/min). After completion of these cycles, the girders were unloaded and the residual deflection was measured. To complete the test, the girders were loaded to 0.40 in. (10.2 mm) of deflection, accounting for residual effects, and cycled for another 100 load-unload cycles at a rate of 4 cycles/min.

The overload behavior measurements are presented in Figure 30. During this portion of ultimate testing, the average peak load applied was calculated as 57.2 kips (254 kN), with an average peak deflection of 1.99 in. (50.5 mm). Figure 30 shows that the girders began to yield at approximately 1.2 in. (30.5 mm) of deflection. Yielding was also observed visually as multiple flexural cracks began to appear and propagate in the nearly pure moment region. The girders were then unloaded at 0.1 in/min (2.54 mm/min) and the residual deflection caused by the ultimate loading was recorded as 0.30 in. (7.62 mm). The girders were once again loaded at 0.1 in/min (2.54 mm/min) to a deflection of 0.40 in. (10.2 mm) past the residual deflection giving a total displacement measurement of 0.7 in. (17.8 mm). The girders were subjected to 100 more load-unload cycles. These final cycles were completed at the service deflection limit and were performed to mimic the load-deflection behavior of a bridge structure that remains in service after an overload situation.

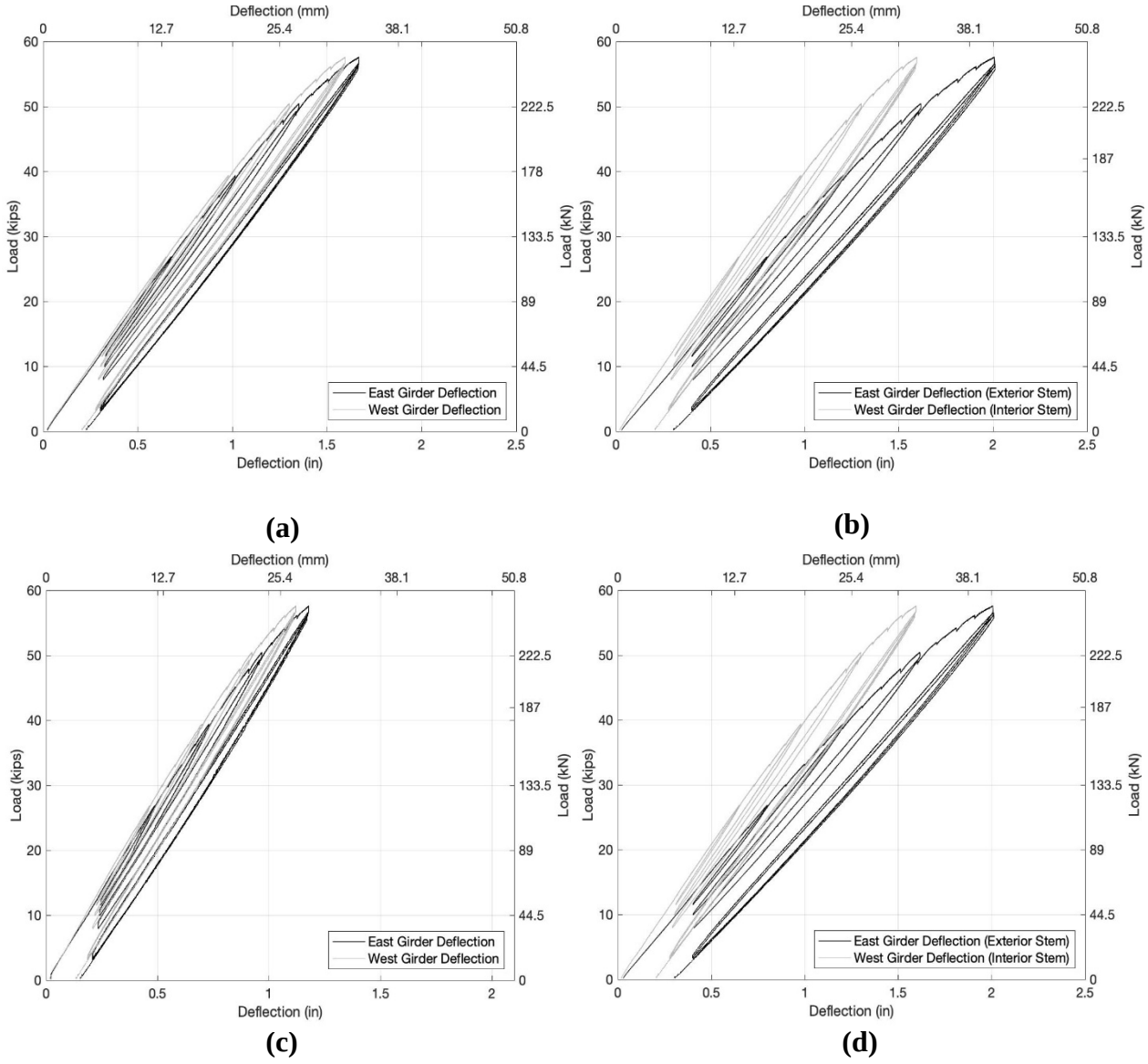

Figure 30. Load versus deflection of east and west adjacent girders for ultimate loading: (a) interior stems of each girder at mid-span (b) exterior stem of east girder and interior stem of west girder (c) interior stems of each girder at first quarter point of span and (d) interior stems of each girder at third quarter point.

Figure 31 presents the load-deflection response for the final 100 load-unload cycles. The final 100 cycles were found to have an average peak applied load of 13.7 kips (60.9 kN), causing an average deflection of 0.68 in. (12.3 mm), including the residual deflection. Once load cycles were complete, it was observed that flexural cracks had propagated in regular intervals across mid-span of both the east and west girders. While the measured vertical displacement had increased, the girders still required approximately the same load to reach a deflection of 0.4 in. (10.2 mm) beyond the 0.3 in. (7.62 mm) of the measured displacement that was permanent. Also, a larger differential displacement between the exterior east girder stem and interior west girder stem was observed after applying the 57.2-kip (254-kN) load, indicating bond damage to the shear key. This reduced

the transfer of shear and moment causing a substantial increase in the deflection of the east girder since the west girder was carrying less of the load.

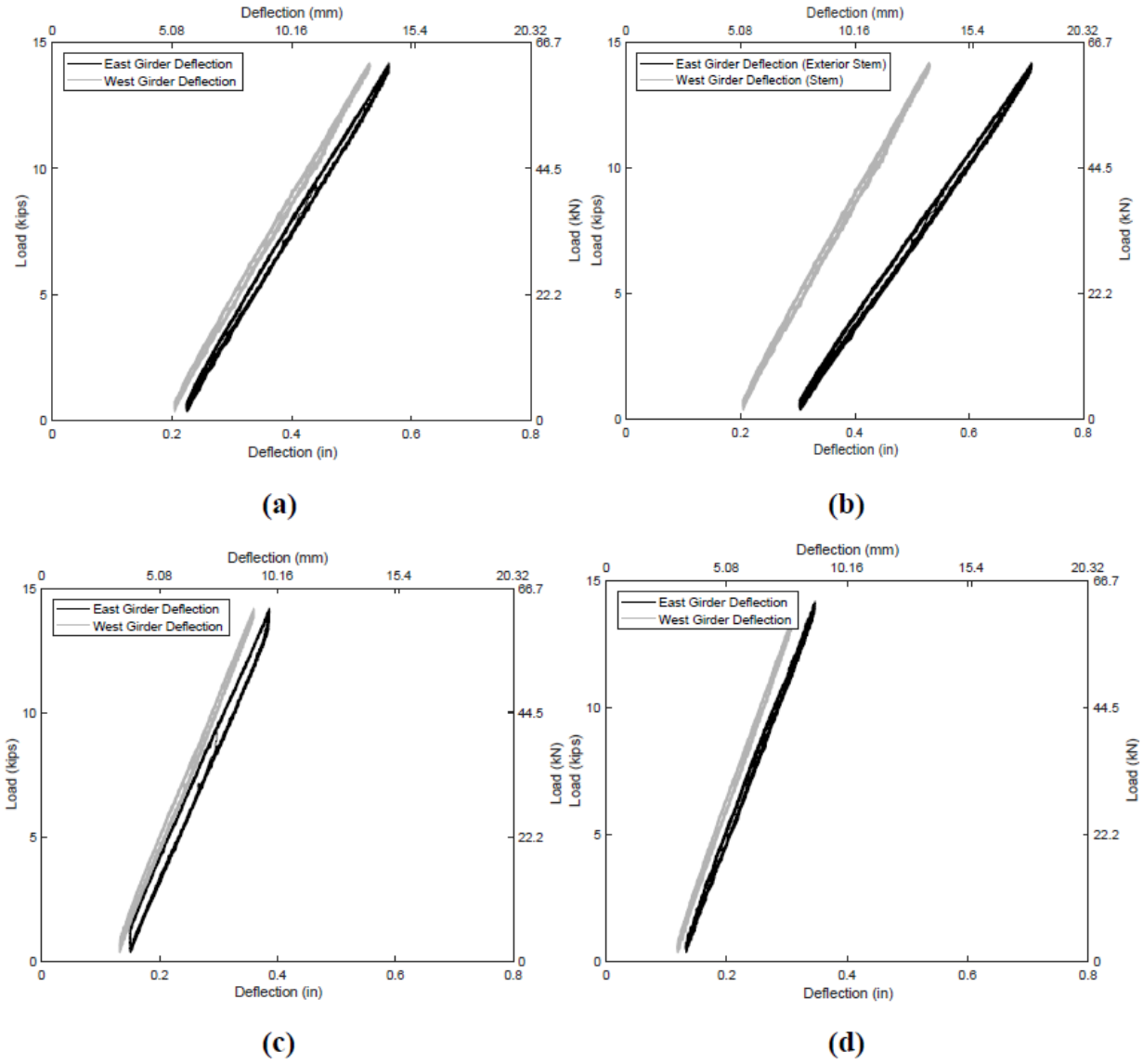

Figure 31. Load versus deflection of east and west adjacent girders for final 100 cycles after ultimate loading: (a) interior stems of each girder at mid-span (b) exterior stem of east girder and interior stem of west girder (c) interior stems of each girder at first quarter point of span and (d) interior stems of each girder at third quarter point.

5.4.4. Moment Distribution Factors

To better understand the behavior of each cyclic test, the shear and moment distribution factors were calculated. This was done by finding the difference between the moment in the east girder at different cycles for the grouted shear key tests (CL1, CL2, and CL4) and the mean moment from the single girder test (CL3). The calculation used to find the moment distribution factors was $DF = \frac{M_2 - M_1}{M_2}$, where M_1 is the average moment obtained for the single girder test (CL3) and M_2 is the average of the moments found at cycle 1, cycle 500, and cycle 1000 for the east girder in the

CL1, CL2, and CL3 tests. The resulting moment distribution factors are presented in Table 8. These results show that the grouting materials performed comparably, and that moment distribution was also influenced by the slight decrease girder stiffness as testing progressed.

Table 8. Shear and moment distribution factors for CL1, CL2, and CL4.

Loading Scenario	Shear and Moment Distribution Factor (DF)
CL1	0.498
CL2	0.440
CL4	0.436

Shear distribution factors were estimated to be equivalent to the moment distribution factors since the ratio of load to deflection on the individual girders is equal to the ratio of moment to deflection and because the flexural responses of the assemblages dominated the overall responses. The equivalence of these ratios is supported by the linear elastic behavior observed during the full-scale tests.

5.4.5. Summary of Ultimate Loading

A summary of load-deflection behavior for cyclic and ultimate loadings of the test girders is provided in Table 9.

Table 9. Summary of load-deflection behavior for all loadings.

Load Scenario	Event	Average Peak Load kips (kN)	Average Peak Deflection in. (mm)
CL1	Maximum	13.9 (61.9)	0.41 (10.4)
CL2	Maximum	13.4 (59.6)	0.40 (10.2)
CL3	Maximum	7.40 (32.9)	0.39 (9.91)
CL4	Maximum	13.2 (58.7)	0.40 (10.2)
UL	Maximum	55.9 (249)	2.00 (50.8)

6. CONCLUSIONS

Based on the research conducted during the course of this project, the following conclusions were drawn from this work:

1. Development of adequate bond strength was achieved at seven days for slant-shear and direct tensile strength tests. However, low bond strengths occurred at 28 days from fractures that occurred in the substrate. Consequently, the low strengths appear to be caused more by the low strength of the substrate, which may have also been compromised by chipping during surface preparation, than a deficiency in the bond between the UHPC and the substrate.
2. Low direct tensile strengths were also obtained for formed surfaces at 28 days. These fractures occurred at the bonded interface, not in the substrate. Additionally, the formed surface was not chipped to provide texture. Consequently, it appears that shrinkage differences between the UHPC and the substrate were the cause of the inadequate bond strength.
3. Shrinkage measurements of the UHPC mixture used in this research were consistent with results from previous research.
4. Early-age shrinkage was substantial (approximately 1600 microstrain at 24 hours). However, the UHPC was still plastic during approximately the first 1000 microstrain of early-age shrinkage. This portion of the shrinkage is unlikely to produce significant stresses on the bonded interface due to the plastic behavior of the UHPC and the low elastic modulus at early ages.
5. Longer-term shrinkage accounted for approximately 450 microstrain of shrinkage in the UHPC. All of this shrinkage is expected to contribute to shear stresses at a bonded interface with mature substrate.
6. Full-scale testing of two channel girder assemblages with UHPC grouted shear keys demonstrated that the bond between the UHPC grout and the mature girders was able to withstand the maximum permissible deflection for an equivalent bridge. This occurred for formed shear key surfaces that provided improper bond (not pre-wetted) as well as full bond (pre-wetted) for the UHPC grout.
7. The excellent bond observed between the UHPC grout and the mature channel girders during full-scale testing occurred with no lateral restraint such as post-tensioning. This indicates that the bond strength between UHPC and mature substrate with a formed surface is not as great a concern as the bond strength results seemed to indicate.
8. During three full-scale tests, two with UHPC grout and one with a commercially available non-shrink grout, the stiffness of the girders was observed to slightly decrease as testing progressed. This behavior did not appear to be caused by any behavior of the shear keys.
9. The non-shrink grout appeared to slightly outperform the UHPC grout. While the structural performance of the non-shrink grout was only marginally better than the performance of the UHPC grout, it does indicate that the UHPC grout does not provide a mechanical benefit over the non-shrink grout. Therefore, if UHPC grout is selected for shear key applications, that decision should be based on durability and possibly economy.

REFERENCES

1. Hussein, H., S. Sargand, and E. Steinberg. Shape Optimization of UHPC Shear Keys for Precast, Prestressed, Adjacent Box-Girder Bridges. *ASCE Journal of Bridge Engineering*, 2018. 23(4): 1-5.

2. Weldon, B.D., D.V. Jauregui, C.M. Newtson, C.W. Taylor, K.F. Montoya, S. Allena, J. Muro, M. Tahat, E. Lyell, and E.T. Visage. *Feasibility Analysis of Ultra-High-Performance Concrete for Prestressed Concrete Bridge Applications.* Report NM09MCS-01, New Mexico Department of Transportation, 2012.

3. Newtson, C.M., B.D. Weldon, A.J. Al-Basha, M.P. Manning, W.K. Toledo, and L.D. Davila. *Bridge Deck Overlays Using Ultra-High-Performance Concrete.* Tran-SET final research report for project 17CNMS01. Transportation Consortium of South-Central States (Tran-SET), 2018.

4. Ozyildirim, C. and G. Moruza. High-Performance Grouting Materials in Shear Keys Between Box Beams. *Transportation Research Record: Journal of the Transportation Research Board*, 2016. Volume: 10.3141/2577-05.

5. Montoya, K. *Feasibility of Using Ultra High Performance Concrete in New Mexico Bridge Girders.* M.S. thesis. New Mexico State University, 2010.

6. ASTM E965: *Measuring Pavement Macrotexture Depth Using a Volumetric Technique.* Annual Book of ASTM Standards. ASTM International, West Conshohocken, PA, 2015.

7. Graybeal, B. *Ultra-High Performance Concrete*. Public FHWA-HRT-11-038. FHWA, U.S. Department of Transportation, 2011.

8. ASTM C1856: *Fabricating and Testing of Ultra-High Performance Concrete.* Annual Book of ASTM Standards. ASTM International, Conshohocken, PA, 2017.

9. Al-Basha, A. *Frost Resistance of Concrete Cladded with Locally Produced Ultra-High-Performance Concrete Cured at Elevated Temperatures.* M.S. thesis. New Mexico State University, 2017.

10. Ubbing, J. *Analytical Investigation of Adjacent Box Beam Ultra-High Performance Concrete Connections.* M.S. thesis. Ohio University, 2014.

11. Villanueva, J.M. *Mixture Proportioning and Freezing and Thawing Durability of Ultra High-Performance Concrete Using Local Materials.* Ph.D. dissertation. New Mexico State University, 2015.

12. Allena, S. and C.M. Newtson. Shrinkage of Fiber-Reinforced Ultra-High Strength Concrete. *ASCE Journal of Materials in Civil Engineering*, 2011. 24(5): 612-614.

13. Lyell, E. *Optimization of Ultra High-Performance Concrete Mixture Proportions using Locally Available Materials.* M. S. thesis. New Mexico State University, 2012.

14. Haber, Z.B., I. De la Varga, B.A. Graybeal, B. Nakashoji, and R. El-Helou. *Properties and Behavior of UHPC-Class Materials.* FHWA-HRT-18-036. FHWA, U.S. Department of Transportation, 2018.

15. Yuan, J. and B. Graybeal. Full-Scale Testing of Shear Key Details for Precast Concrete Box-Beam Bridges. *ASCE Journal of Bridge Engineering,* 2016. 21(9): 1-13.

16. Attanayake, U. and Aktan, H. First-Generation ABC System, Evolving Design, and Half a Century of Performance: Michigan Side-by-Side Box-Beam Bridges. *ASCE Journal of Performance of Constructed Facilities,* 2015. 29(3): 1-13.

17. Miller, R.A., G.M. Hlavacs, T. Long, and A. Greuel. Full-Scale Testing of Shear keys for Adjacent Box Girder Bridges. *PCI Journal,* 1999. 44(6): 80-90.

18. Sharpe, G. *Reflective Cracking of Shear Keys in Multi-Beam Bridges.* M. S. thesis. Texas A&M University, 2007.

19. Grace, B.F., E.A. Jensen, and M.R. Bebawy. Transverse Post-Tensioning Arrangement for Side-by-Side Box-Beam Bridges. *PCI Journal,* 2012. 57(2): 48-63.

20. Hanna, K.E., G. Morocous, and M.K. Tadros. Transverse Post-Tensioning Design and Detailing of Precast, Prestressed Concrete Adjacent-Box-Girder Bridges. *PCI Journal,* 2009. 56(4): 160-174.

21. El-Remaily, A., M.K. Tadros, T. Yamane, and G. Krause. Transverse Design of Adjacent Precast Prestressed Concrete Box Girder Bridges. *PCI Journal,* 1996. 41(4): 96-113.

22. Annamalai, G. and R.C Brown. Shear Strength of Post-Tensioned Grouted Keyed Connections in Precast Concrete-Framed Structures. *ACI Structural Journal,* 1990. 87(1): 53-59.

23. Graybeal, B. *Design and Construction of Field-Cast UHPC Connections.* Public FHWA-HRT-14-084. FHWA, U.S. Department of Transportation, 2014.

24. ACI 546: *Guide for the Selection of Materials for the Repair of Concrete.* American Concrete Institute, Farmington Hills, MI, 2004.

25. ICRI 310. Committee 310. *Selecting and Specifying Concrete Surface Preparation for Sealers, Coatings, Polymer Overlays, and Concrete Repair.* ICRI310.2R-2013. International Concrete Repair Institute, 2013.

26. Badie, S., M. Tadros, and A. Girgis. *Full-depth, Precast-Concrete Bridge Deck Panel Systems.* NCHRP 12-65. National Cooperative Highway Research Program, 2006.

27. Issa, Mo.A., C.L. Ribeiro do Valle, H.A. Abdalla, S. H. Islam, and Ma.A. Issa. Performance of Transverse Joint Grout Materials in Full-Depth Precast Concrete Bridge Deck Systems. *PCI Journal*, 2003. 48(4): 92-103.

28. Miller, R.A., G.M. Hlavacs, T. Long, and A. Greuel, Full-Scale Testing of Shear Keys for Adjacent Box Girder Bridges. *PCI Journal,* 1999. 44(6): 80-90.

29. Gulyas, R.J., G.J. Wirthlin, and J.T. Champa, Evaluation of Keyway Grout Test Methods for Precast Concrete Bridges. *PCI Journal,* 1995. 40(1): 44-57.

30. Joyce, P.C. *Development of Improved Connection Details for Voided Slab Bridges.* M.S. Thesis. Virginia Polytechnic Institute, 2014.

31. Hussein, H.H., S.M. Sargand, F.T. Al Rikabi, and E.P. Steinberg. Laboratory Evaluation of Ultra High-Performance Concrete Shear Key for Prestressed Adjacent Precast Concrete Box Girder Bridges. *ASCE Journal of Bridge Engineering,* 2017. 22(2):1-12.

32. ASTM C882 / C882M: *Standard Test Method for Bond Strength of Epoxy-Resin Systems Used With Concrete By Slant Shear.* Annual Book of ASTM Standards. ASTM International, West Conshohocken, PA, 2013.

33. ASTM C1583: *Tensile Strength of Concrete Surfaces and the Bond Strength or Tensile Strength of concrete Repair and Overlay Materials by Direct Tension (Pull-off Method).* Annual Book of ASTM Standards. ASTM International, West Conshohocken, PA, 2013.

34. BS 1881: *Testing Concrete Part 116: Method for Determination of Compressive Strength of Concrete Cubes.* British Standards Institution (BSI). 1991.

35. ASTM C39: *Standard Test Method for Compressive Strength of Cylindrical Concrete Specimens.* Annual Book of ASTM Standards. ASTM International, West Conshohocken, PA, 2018.

36. Holt, E.E. *Early Age Autogenous Shrinkage of Concrete.* VTT publication 446. Technical Research Centre of Finland, 2001.

37. Lozoya, J. and C.M. Newtson. Effects of Early Misting on Concrete Shrinkage. Proceedings: Advancing Concrete Through Science and Engineering. RILEM, 2004.

38. ASTM C157: *Length Change of Hardened Hydraulic-Cement Mortar and Concrete.* Annual Book of ASTM Standards. ASTM International, Conshohocken, PA, 2017.

39. *LRFD Bridge Design Specifications.* 6th ed. American Association of State Highway and Transportation Officials (AASHTO), Washington, D.C., 2012.